

We are grateful to the reviewers for their time and constructive comments to improve this manuscript. Here we address our reply point by point, in bold font. Reviewer's comments are in regular font. All changes are marked with red in the revised manuscript.

Reviewer 1:

This paper uses altimetry and bathymetry data to map changes in the grounded area of the Mertz ice tongue during the early-to-mid 2000s. They use the surface heights of lightly-grounded icebergs to estimate the firn air content for the ice tongue, and use this, geoid-corrected altimetry measurements, and a bathymetry map of the ice shelf, to map the difference between the bottom of the ice shelf, at hydrostatic equilibrium, and the sea bed for different time periods. Areas where these maps show the (hydrostatic) ice bottom below the seabed are treated as grounded. The authors find that the northwest flank of MIT (Mertz Ice Tongue) was grounded during 2002-08, and that the grounding increased between 11/2004 and 12/2006. They propose that the MIT would have calved because of increasing grounding extent even if the tongue had not been hit by an iceberg. The authors also examine the rate of change in the area of MIT, and estimate an interval between subsequent tongue calving events of 70 years.

A quick summary of this review is that this manuscript needs a great deal of editing and extensive revision before it is ready for publication. I have presented some of my thoughts about what needs to be fixed, but the writing is of uneven quality and my comments about the reliability of interpolated data should (in my opinion) lead to substantial changes in the text and figures. With this in mind, I have not gone to the effort of editing the paper in detail, and hope that the authors can do so themselves.

Reply: Thank you for your comments. We have made many revisions to the structure. Please find related changes highlighted in red in the text.

A major problem in this manuscript is the lack of bathymetry data under the MIT. Data are scattered, at varying density, seaward of the ice front, and the bathymetry maps appear to resolve the seaward extent of the Mertz Bank, but under the tongue the maps are entirely based on interpolated values. This makes the maps in figure 5 and the statistics in table 2 hard to believe except at the very edge of MIT where the altimetry and bathymetry more or less coincide. The conclusions of the paper are largely independent of the data everywhere except in the area where the data are credible, which makes me wonder why the authors chose to show the mapped elevation-difference values in the areas for which they have no data. The authors should make a clear distinction between results derived from measurements and results derived from interpolated values, and the relative expected accuracies of each.

Reply: Through further reading the references about GEBCO and ETOPO1 seafloor DEM, we do find there exists a bathymetry data gap under the MIT as the reviewer has pointed out. According to Beaman et al. (2011), the oldest bathymetry data collected along the margin of the MIT was at least from 2000. Thus, the boundary of the MIT in 2000 is used to identify bathymetry measurement gaps, as is indicated in Fig. 6. We want to use this boundary to identify the different quality of the seafloor DEM data.

As far as we know, there are no other new bathymetry measurements which can be used to verify the region of data gaps. Thus a further validation of the seafloor DEM is not conducted. Luckily, the ice tongue moved further into the ocean from 2000 to 2010 before calving, flowing over seafloor where bathymetry measurements density is good. Furthermore, the grounding detected is all located beyond the 2000 MIT boundary. Thus the analysis of grounding detection near the ice front in 2002, 2004, 2006 and 2008 is convincing. In this revision, the grounding detection result from Fig. 6 (Fig. 5, last version) is unchanged. However, the boundary of MIT in 2000 is now added to separate the seafloor area under the MIT where the seafloor was interpolated from the surrounding area where bathymetry measurements have been made. The statistical result of grounding detection in Table 2 is recalculated accordingly. Detailed discussion on the seafloor DEM is added in a newly added section 6.2.3.

A second problem is that the methods are difficult to interpret, in large part because the report cited as “Wang 2014” is not readily available online, and the paper “Wang et al 2014” appears to describe a method for estimating freeboard change, rather than the absolute freeboard used in the present study. A good deal of the material in this paper is based on a technique in that report, described briefly in section 3.1(126-135). This paper should include a full description of the technique. In particular, it is not clear from the description how the relocation step works or what it is supposed to accomplish, or how the surface slope relates to errors in this relocation (line 241). I would also have liked to see a justification for the kriging interpolation between ICESAT profiles; the grounding features appear to be small compared to the gaps between ICESAT tracks, which makes me suspect that the krigged freeboard values may not provide a good indication of grounding.

Reply: For freeboard production, we did not cite Wang 2014, but Wang et al. 2014, which did show how to use ICESat/GLAS data to produce a freeboard map in 2009 before MIT calving. In the revision, more details on the freeboard production method are given in Section 3.1. Uncertainty of kriging interpolation using ICESat/GLAS data is investigated as well which is about ± 1.8 m on average in a new Section 4.1. The uncertainty of kriging interpolation is also considered when calculating the final grounding detection accuracy in Section 4.

The authors should also be clear about the tidal values used in the freeboard study. Are the altimetry values corrected for tides? What is the “lowest sea level” mentioned at 155, and elsewhere? Is it derived from a tide model, or is it the lowest observed sea level? Is the tide model on the ICESAT product used, or is a different tide model used? What are the errors involved in each part of this?

Reply: More details on ICESat/GLAS preprocessing and the method to produce the freeboard map has been given in the revised text. Tide correction of ICESat/GLAS GLA12 from TPX07.1 is removed to obtain the instantaneous sea surface condition. “lowest sea level” in line 155 may be confusing and has been changed to “lowest sea surface height among extracted sea surface height from different tracks and different campaigns, which is -3.35 m”. It is derived by comparing all sea surface height derived from different tracks and campaigns from 2003 to 2009, not from a tide model. The lowest sea surface height stands for the lowest sea level around Mertz from 2003 to 2009 and is directly from ICESat/GLAS observation. Sea level lower than -3.35 m may in fact exist over the Mertz region since limited ICESat observation in any year may not catch the lowest one. The influence of sea level -3.35 m used in this study is discussed more in a new Section 6.2.1.

The English in the manuscript needs improvement. A few idioms are used throughout that are confusing or distracting. “Inversed” should be “inverted.” “Area-changing rate” should just be “area rate.” “Least-square” should be “least-squares.” Activities in the current study should be in present tense, citations to the literature should be in past tense.

Reply: These grammatical issues have been resolved. The error or uncorrected expression pointed to by the reviewer has been corrected. More unclear descriptions or grammar misuses have been corrected as indicated in red in the revised text.

The FAC calculation (3.2) has some nice features, but needs to be described in more detail. How is the least-squares inversion carried out? What are the error sources?

Reply: More details about FAC calculation have been given. Please read Section 3.2 and 6.2.2.

160-177- is the extensive discussion of other methods of calculating the FAC germane to this study? This section would be clearer if much of this were omitted.

Reply: The introductory part of Section 3.2 has been revised. One paragraph not related to the FAC calculation much has been removed. Please read the revised Section 3.2.

222-229- this paragraph should be in the introductory part of section 3.2, not after the calculations have been presented.

Reply: In the introductory part of Section 3.2, the principle of FAC has been given. However, we want to use this text to discuss limitations of the FAC as calculated from these selected icebergs. In the revision, this paragraph in question is now moved to Section 6.2.2 as part of a deeper discussion on FAC extraction.

247: Where are the interpolation errors for freeboard and bathymetry?

Reply: The influence of kriging interpolation is discussed in Section 4.1. Also the uncertainty of kriging interpolation is derived and now considered in the final accuracy of grounding detection.

From Beaman et al. (2011), the poorest accuracy of single beam and multi-beam measurements was provided. Thus, we use it directly to evaluate the accuracy of the data in Section 4.1. Because the original bathymetry data product from Beaman et al. (2011) and Fretwell et al. (2013) was not collected and processed by us, it is impossible to evaluate the uncertainty of the products. As far as we know, there is no other new bathymetry measurements that can be used to evaluate the seafloor DEM. Thus, for seafloor DEM, we just use the poorest accuracy to reflect the uncertainty of seafloor DEM. The seafloor DEM is further discussed in a new Section 6.2.3.

254- 50 times the average slope is still a very small number (0.6 degrees). A better estimate of the error due to crevassing would be to directly incorporate the crevasse depth into the calculation- thus, instead of $v \cdot \text{slope_error}$ (12 m) the contribution would be closer to 50 m.

Reply: Crevasses are important features on the surface of the MIT. In the middle of the tongue, large crevasses can reach a depth of about 50 m. However, this is an extreme and rare occurrence. Around the ice front, the freeboard is about 30 m, as can be seen from Wang et al. (2014). It is therefore not proper to set the crevasse depth in that area to be as large as 50 m. The freeboard error caused by our approach is reasonable because we want to explore the average contribution to grounding detection from footprint relocation by considering ice velocity uncertainty and average surface slope. In this study, we have already magnified it by 50 times. As we feel this is a reasonable approach for the ice front treatment, we kept our original approach in the revised manuscript.

256-62: Why do we need to consider the freeboard stable (or not stable?) It appears that only static estimates of freeboard are used here (derived from single ICESAT campaigns)- so why does it matter that there would be a change (or not) in the freeboard?

Reply: Greater details about the method for freeboard extraction, relocation and mapping are added in Section 3.1. Because we use all ICESat/GLAS data from 2003 to 2009 to produce freeboard for different years, freeboard changes do matter if freeboard changed greatly. Thus,

the uncertainty of freeboard change rate does contribute to the final accuracy of grounding detection.

257 “annual changing rate of freeboard” should be “annual rate of freeboard change” or “freeboard rate”

Reply: Done

273: What is the significance of $E_{dif} < 34$ m? Based on 263-268, this would indicate “not extremely confidently identified as ungrounded.” Wouldn’t a better statistic be $E_{dif} < -34$, or “Extremely confidently identified as ungrounded?”

Reply: After considering the interpolation error, the accuracy for grounding detection is now ± 23 m (± 17 m in last version). We provide statistics for those elevation difference with E_{dif} less than 46 m (twice the standard deviation) so one can have a better estimate of grounding at the tongue. When using E_{dif} less than -46 m, the slightly grounded sections will be neglected. We use this value of 46 m to describe all possible grounding regions. Furthermore, the statistics in Table 2 do show results in different intervals from 46 m to less than 0.

280: Again: Do you mean “less than -17 m?”

Reply: We mean “less than 23 m” because in 2002, the minimum of ‘ E_{dif} ’ is larger than “-23 m”. In this revision, ‘17’ is changed to ‘23’ because of a revised consideration of the kriging interpolation error.

291-293: Reporting E_{dif} within the tongue is a problem, since the bathymetry is not known there. You might report changes along the margin, but the statistics reported here don’t seem to mean anything.

Reply: We actually want to express the ‘ E_{dif} ’ for those regions listed in Table 2 only, not all regions under the tongue. These regions with ‘ E_{dif} ’ less than 46 m do fall beneath the ice front of the MIT. In this revision, we change it to “From 2002 to 2008, more regions under the MIT have ‘ E_{dif} ’ less than 46 m the area of which increased from 8 km² to 17 km². Additionally, the mean of ‘ E_{dif} ’ under the tongue for those having ‘ E_{dif} ’ less than 46 m gradually decreases from 28.8 m to 12.3 m, according to which we can conclude that the ice front was grounded more significantly with passing time. ”

302 Combine the first two sentences, which form a joint conclusion: “. However,” should be “, and that”

Reply: Done.

325 (and elsewhere) “Area-expanding trend” should be “area rate” or “rate of area change”

Reply: Done.

367-78: The significance of this paragraph is not clear. Ice-berg scouring is not discussed elsewhere in the paper, so the scientific question addressed by this paragraph needs more introduction.

Reply: This section is removed.

577- “is used in figure 6”– this appears not to be true.

Reply: Changed it to ‘Fig. 4’

589: “closed’ – should this be “closest?”

Reply: Done.

594: The legend here is not consistent with the caption.

Reply: Legend is changed.

606: It is hard to distinguish the outline from the “grounding part.” The choice of colors (yellow on yellow) is not good.

Reply: This figure is redrawn and yellow lines are not used in this version.

Reviewer 2:

The authors use bathymetric, ICESat, and Landsat data products to estimate the firn air content, depth below sea level, re-grounding locations, and advance rate for the Mertz Ice Tongue from 2002-2008. They find that grounding along the Mertz Bank resulted in slight rotation and rifting of the Mertz Ice Tongue that would have resulted in the ice tongue's eventual collapse in the absence of any additional triggering mechanisms. Further, they suggest that the ice tongue collapse has a periodicity of ~70 years and that this periodicity results in periodic variations in local sea ice formation and bottom water formation. Although the topic of the manuscript is interesting, the limited presentation of the methods and irregular quality of the writing make it difficult to follow. In addition to the major revisions listed below, I recommend that the authors go through the text in detail to check the writing and to make sure that all figures are legible.

Reply: Thanks for your comments. We have thoroughly revised the manuscript. The changes are highlighted in red in the revised text.

1) In the data and methods sections, the authors frequently refer the readers to other publications rather than describe the data processing procedures in detail in the text. I find this to be particularly concerning for the freeboard inversions to estimate ice thickness because small errors in freeboard can lead to large variations in the estimated tongue depths. In order to have confidence in the provided tongue depths, I recommend including more detail on the relocation and interpolation procedures. Similarly, more information regarding the uncertainty of the bathymetry data used to identify grounded regions would be incredibly helpful.

Reply: More details about freeboard map production using all available ICESat/GLAS data from 2003 to 2009 is added in a revised Section 3.1. More discussion is added as well in a new Section 6.2.3.

From Beaman et al. (2011), the poorest accuracy of single beam and multi-beam measurements was provided. Thus, we use it directly to evaluate the accuracy of this data in Section 4. Because the original bathymetry data product from Beaman et al. (2011) and Fretwell et al. (2013) was not collected and processed by us, it is impossible to fully evaluate the uncertainty of the products. The seafloor DEM is further discussed in the new Section 6.2.3.

We do acknowledge that in regions with bathymetry gaps, the quality of seafloor topography is poorer compared to other regions. According to Beaman et al. (2011), the oldest bathymetry data used to produce the seafloor DEM that are already known was at least from 2000. Thus, the boundary of the MIT in 2000 is used to identify bathymetry measurement gaps, as is indicated in Fig. 6. We use this boundary to identify the different quality of the seafloor DEM data since as far as we know, there is no other new bathymetry measurements

that can be achieved to verify the region of data gaps. Luckily, the ice tongue moved further into the ocean from 2000 to 2010, before calving, into regions where bathymetry measurements are good. Furthermore, the grounding we detect is all located beyond the 2000 MIT boundary. Thus the analysis of grounding detection near ice front in 2002, 2004, 2006 and 2008 is convincing.

2) It's really difficult to follow the firn air content approximation. I assume the bed elevations are really well constrained under the targeted icebergs and you are simply iteratively estimating the iceberg depths for gradually decreasing values of the mean iceberg density. The units obtained for the firn air content estimated using this method require explanation. I assume that they represent the difference in iceberg depth assuming a constant ice density and the final ice density estimated through the comparison with the underlying bathymetry since the units are in meters, but this is not presented anywhere. It would be helpful to also present the final density inferred for the firn column so that it is easier to compare your estimates with other observations. The error estimates obtained for firn air content should also be presented in more detail. I am particularly concerned with the assumption that the ICESat tracks capture the thickest portion of each iceberg. I'd be more confident in the firn air content estimates if I was also shown that there are relatively small variations in iceberg freeboard along the ICESat tracks because that would increase confidence that the iceberg grounding location is captured by the ICESat data.

Reply: The method for FAC calculation has been revised in Section 3.2. The seafloor DEM is well controlled by the bathymetry measurements as can be seen from S-Fig. 1. A paragraph on why FAC is used and how it is obtained is provided in Section 3.2. Some text not related so much to FAC calculation has now been removed. Fig. 9 is added to show the spatial distribution of freeboard of icebergs. More details on freeboard measurements from ICESat/GLAS, and the limitation of our method for FAC calculation is discussed in Section 6.2.2. Our estimated FAC around Mertz is compared with published modeling results (from Ligtenberg, 2014) in Section 6.2.2. Calculating the average density directly is beyond the scope of the current manuscript.

3) The addition of the iceberg scour section at the end of the discussion is somewhat out of place with the rest of the manuscript. I suggest removing it entirely.

Reply: This section is removed.

1 **Grounding and Calving Cycle of Mertz Ice Tongue**

2 **Revealed by Shallow Mertz Bank**

3 Xianwei Wang^{1,2}, David M. Holland^{2,3}, Xiao Cheng^{1,5} and Peng Gong^{4,5}

4 1. State Key Laboratory of Remote Sensing Science, and College of Global Change and Earth System Science,

5 Beijing Normal University, Beijing 100875, China.

6 2. Center for Global Sea Level Change, New York University Abu Dhabi, Abu Dhabi, United Arab Emirates.

7 3. Courant Institute of Mathematical Sciences, New York University, New York 10012, United States of America.

8 4. Ministry of Education Key Laboratory for Earth System Modeling, and Center for Earth System Science,

9 Tsinghua University, Beijing, China 100084.

10 5. Joint Centre for Global Change Studies, Beijing, China.

11
12 *Correspondence to: wangxianwei0304@163.com*

13 **Abstract**

14 A recent study, using remote sensing, provided some evidence that a seafloor shoal
15 influenced the 2010 calving event of the Mertz Ice Tongue (MIT), by partially grounding the
16 MIT several years earlier. In this paper, we start by proposing a method to calculate ~~firn~~ Firn air
17 Air content ~~Content~~ (FAC) around Mertz from seafloor-touching icebergs. Our calculations
18 indicate the FAC around Mertz region as 4.87 ± 1.31 m. We then design an indirect method of
19 using freeboard and sea level data extracted from ICESat/GLAS, FAC, and ~~highly~~ relatively
20 accurate seafloor topography to detect grounding sections of the MIT between 2002 and 2008
21 and analyze the process of grounding ~~before~~ prior to the calving event. By synthesizing remote
22 sensing data, we point out that the grounding position was ~~just~~ localized northeast of the Mertz
23 ice front close to the Mertz Bank. The grounding outlines of the tongue caused by the Mertz
24 Bank are extracted as well, ~~however the length is only limited in several kilometers since late~~
25 2002. From 2002 to 2008, the grounding area increased and the grounding became more
26 pronounced. Additionally, the ice tongue could not effectively climb over the Mertz Bank in
27 following the upstream ice flow direction and that is why MIT rotated clockwise after late 2002.
28 Furthermore, we demonstrate that the area-increasing trend of the MIT changed little after
29 calving ($\sim 36 \text{ km}^2/\text{a}$), thus allowing us to use remote sensing to estimate the elapsed time until the
30 MIT can reground on the shoal. This ~~time~~ period is approximately 70 years. The calving of MIT
31 can be ~~repeatable~~ cyclical because of the shallow Mertz Bank location and the flow rate of the
32 tongue. ~~and~~ The calving cycle of the MIT explains the cycle of sea-surface condition change
33 around the Mertz.

34 **Keywords:** Mertz Ice Tongue, ~~Firn~~ firn air content, iceberg grounding, Mertz Bank, iceberg
35 scouring, calving cycle.

36 **1. Introduction**

37 Surface-warming induced calving or disintegration of floating ice has occurred in
38 Antarctica, such as the Larsen B ice shelf (Scambos et al., 2000, 2003; Domack et al., 2005;
39 Shepherd et al., 2003). While surface or sub-surface melting has largely been recognized to
40 contribute to floating ice loss in Antarctica (Depoorter et al., 2013), calving caused by interaction
41 with the seafloor has not been widely considered. The Mertz Ice Tongue (MIT) was reported to
42 have calved in 2010, subsequent to being rammed by a large iceberg, B-9B (Legresy et al. 2010).
43 After the calving, the areal coverage of the Mertz polynya, and sea-ice production and dense,
44 shelf-water formation in the region changed (Kusahara et al. 2011; Tamura et al. 2012). However,
45 the iceberg collision may have only been an apparent cause of the calving as other factors had
46 not been fully considered such as seafloor interactions (Massom et al., 2015; Wang. 2014). By
47 comparing ~~inversed~~-inverted ice thickness to surrounding bathymetry, and combining remote
48 sensing, Massom et al., (2015) considered that the seabed contact may have held the glacier
49 tongue in place to delay calving by ~8 years. The interaction of the MIT ~~and-with the~~ seafloor,
50 the exact grounding location of the MIT before calving and how severe the grounding was are
51 still not well-known.

52 The MIT (66 S-68 S, 144 E-150 E, Fig. 1) is located in King George V Land, East
53 Antarctica, with an ice tongue extending over 140 km from its grounding line to the tongue front
54 and approximately 30 km wide at the front (Legresy et al., 2004). Much field exploration has
55 been conducted around Mertz and ~~the~~ increasing availability over the last decade of remote
56 sensing, hydrographic surveying, and bathymetric data allow the causes of ice tongue instability
57 to gradually come into focus. From satellite altimetry, a modest elevation change rate of 0.03 m/a
58 (Pritchard et al., 2012) and a freeboard change rate of -0.06 m/a (Wang et al., 2014) were found,

59 which implied that the combined effects of surface accumulation and basal melt were not
60 dramatic for this ice tongue. For the MIT, investigations of tidal effects, surface velocity, rift
61 propagation, and ice front propagation (Berthier et al., 2003; Frezzotti et al., 1998; Legresy et al.,
62 2004; Lescarmonier et al., 2012; Massom et al., 2010, 2015) have been conducted with an
63 objective of detecting underlying factors affecting stability. Grounding as a potential factor can
64 affect the stability of an ice tongue, as recently pointed out by Massom et al. (2015). However,
65 without highly accurate bathymetric data, it is impossible to carry out such study. Fortunately, In
66 | 2010, a new and high resolution bathymetry model, [for the seafloor surrounding the Mertz](#), with
67 | a resolution of 100 m was released for the Terra Adelie and George V continental margin
68 | (Beaman et al., 2011), and incidentally later used to generate the Bedmap-2 (Fretwell et al.,
69 | 2013). Such accurate data provides an opportunity for better exploring seafloor shoals and their
70 | impact on the instability of MIT. In this study, we focus on the grounding event of the MIT from
71 | 2002 to 2008. A method for grounding event detection ~~will be~~ proposed and the grounding of
72 | the MIT before calving ~~will be~~ investigated. [A calving cycle of the MIT caused by grounding is](#)
73 | [discussed as well](#).

74 **2. Data**

75 | The primary data used [to investigate ice tongue grounding](#) in this study are Geoscience
76 | Laser Altimeter System (GLAS) data onboard the Ice, Cloud and Land Elevation Satellite
77 | (ICESat) and the seafloor bathymetry data mentioned above. In this section, ICESat/GLAS and
78 | bathymetry data, as well as some preprocessing are introduced.

79 **2.1 ICESat/GLAS**

80 | The ~~Ice, Cloud, and Land Elevation Satellite~~ (ICESat) is the first spaceborne laser
81 | altimetry satellite orbiting the Earth, lunched by National Aeronautics and Space Administration

82 | (NASA) in 2003 (Zwally et al. 2002) with ~~Geoscience Laser Altimetry System (GLAS)~~ as the
83 | primary payload onboard. ICESat/GLAS was operated in an orbit of ~600 km and had a
84 | geographical coverage from 86 °S to 86 °N. ICESat/GLAS usually observed in nadir viewing
85 | geometry and employed laser pulses of both 532 nm and 1064 nm to measure the distance from
86 | the sensor to the ground (Zwally et al. 2002). On the ground, ICESat/GLAS's footprint covered
87 | an area of approximately 70 m in diameter, with ~~two~~ each adjacent footprints spaced by ~170 m.
88 | The horizontal location accuracy of the footprint ~~is~~ was about 6 m (Abshire et al. 2005). The
89 | accuracy and precision of ICESat/GLAS altimetry data ~~are~~ were 14 cm and 2 cm respectively
90 | (Shuman et al. 2006). ICESat/GLAS usually ~~observed~~ made two or three campaigns a year from
91 | 2003 to the end of 2009, with each campaign lasting for about one month. With billions of laser
92 | footprints received by the telescope, 15 types of data were produced for various scientific
93 | applications, named as GLA01, GLA02, ... GLA15. In this study, GLA12 data (elevation data
94 | for polar ice sheet) covering the Mertz from release 33 during the interval of 2003 to 2009 is
95 | used, the spatial distribution of which is shown in Fig. 2.

96 | **2.2 Seafloor Topography**

97 | Detailed bathymetry maps are fundamental spatial data for marine science studies
98 | (Beaman et al., 2003, 2011) and crucially needed in the data-sparse Antarctic coastal region
99 | (Massom et al. 2015). Regionally, around Mertz, a large archive of ship track single-beam and
100 | multi-beam bathymetry data from 2000 to 2008 were used to generate a high resolution Digital
101 | Elevation Model (DEM), the spatial coverage of which can be found in Fig. 2 of Beaman et al.
102 | (2011) and bathymetry data coverage over the Mertz region can be found from S-Fig. 1. The
103 | DEM product was reported as having a vertical accuracy of about 11.5 m (500 m depth) and
104 | horizontal accuracy of about 70 m (500 m depth) in the poorest situation (Beaman et al. 2011).

105 Around Antarctica, seafloor topography data from Bedmap-2 was produced by Fretwell et al.
106 (2013) which adopted the DEM from Beaman et al. (2011). In this study, Bedmap-2 seafloor
107 topography data covering Mertz is employed to detect the contact between seafloor and the MIT.
108 Because of inconsistent elevation systems for ICESat/GLAS and seafloor topography data, the
109 Earth Gravitational Model 2008 (EGM08) geoid with respect to World Geodetic System 1984
110 (WGS-84) ellipsoid is taken as reference. Since seafloor topography from Bedmap-2 is
111 | referenced to the so-called g104c geoid, an elevation transformation is required and can be
112 | implemented through Eq. (1).

$$113 \quad E_{sf} = E_{seafloor} + gl04c_{to_wgs84} - EGM2008 \quad (1)$$

114 where ' E_{sf} ' and ' $E_{seafloor}$ ' is the seafloor topography under EGM08 and g104c respectively,
115 ' $gl04c_{to_wgs84}$ ' is the value needed to convert height relative to g104c geoid to that under WGS-
116 84, and ' $EGM2008$ ' is the geoid undulation with respect to WGS-84.

117 3. Methods

118 3.1 Grounding Detection Method

119 ICESat/GLAS data has been widely used to determine ice freeboard, or ice thickness,
120 since its launch in 2003 (Kwok et al., 2007; Wang et al., 2011, 2014; Yi et al., 2011; Zwally et
121 | al., 2002, 2008). To study ice freeboard, draft, and grounding of the MIT in different
122 | years through time, ICESat/GLAS GLA12 data from release 33 from 2003 to 2009 are used as
123 | mentioned, and the spatial coverage of which can be seen in Fig. 2. The methods we designed for
124 | grounding detection of the MIT are now introduced briefly. First, assuming a floating ice tongue,
125 | based on freeboard data extracted in different observation dates, the ice draft of the MIT is
126 | inversed inverted. Next, ice bottom elevation is calculated based on the inversed inverted ice
127 | draft and the lowest sea-sca-surface height. Finally, the ice bottom is compared with seafloor

128 ~~topography-bathymetry~~ and ice grounding is detected. The underlying logic for grounding
129 detection is that if the ~~inversed-inverted~~ ice bottom is lower than seafloor, we can ~~deny the~~
130 ~~former assumption and~~ draw a conclusion that the ice tongue is grounded rather than floating.

131 The method to extract a freeboard map using ICESat/GLAS from multiple -campaigns
132 over the MIT was described in Wang et al. (2014). Here, we ~~will not do not~~ revisit it in detail but
133 introduce it schematically. ~~According to Wang et al. (2014), four-Four~~ steps ~~were-are~~ included
134 in freeboard map production for each of November 14, 2002, March 8, 2004, December 27, 2006
135 and January 31, 2008.extraction.

136 The first step ~~was-is~~ on data preprocessing, saturation correction, data quality control, and
137 tidal correction removal. The magnitude of the ICESat/GLAS waveform can become saturated
138 because of different gain setting, or the occurrence of cloud. Thus the saturated waveforms with
139 'i_satElevCorr' (i.e. an attribute from GLA12 data record) greater than or equal to 0.50 m are
140 ignored and those with 'i_satElevCorr' less than 0.50 m are corrected by adding the correction
141 back (Wang et al. 2012, 2013). Additionally, measurements with 'i_reflectUC' greater than or
142 equal to one are ignored. Furthermore, tidal correction from TPX07.1 tide model in GLA12 data
143 record is removed to ~~get-obtain~~ elevation data on the instantaneous sea surface condition.
144 Finally, elevation data under WGS-84 ellipsoid and EGM 08 geoid for ICESat/GLAS from 2003
145 to 2009 is prepared for subsequent use.

146 The second step ~~was-is~~ to derive sea-level height according to each track and to calculate
147 freeboard for each campaign. Because of tidal variations near the MIT, surface elevations of the
148 MIT can vary as well. To derive sea-level height from ICESat/GLAS and provide a reference for
149 freeboard calculation for different campaigns, ICESat/GLAS data over the MIT within a buffer
150 region (with 10 km as buffer radius of MIT boundary in 2007) are selected and sea-level height

Formatted: Font: Italic

Formatted: Font: Not Italic

Formatted: Font: Italic

151 is determined as the lowest elevation measurement along each track (Wang et al. 2014).
152 Freeboard is then calculated by subtracting the corresponding sea-level height from elevation
153 measurement of the MIT according to different tracks even in the same campaign. Thus
154 freeboard data for different campaigns from 2003 to 2009 is obtained.

155 The third step ~~was~~is to relocate footprints ~~with~~using estimated ice velocity. ICESat
156 observed the MIT almost repeatedly along the same track in different campaigns (Fig. 2).
157 However, observation from only one campaign cannot provide good coverage of the MIT, which
158 drives us to combine all observations from 2003 to 2009 together to produce a freeboard map of
159 MIT. Fig. 2 shows the spatial coverage of ICESat/GLAS from 2003 to 2009 over the Mertz, but
160 the geometric relation between tracks is not correct over the MIT because the tongue was fast
161 moving and observed in different years by the ICESat. The region observed in an earlier
162 campaign would move downstream later (Wang et al. 2014). For example, ICESat collected data
163 from track T31 on March 22, 2003 and T165 (Fig. 2) on November 1, 2003 respectively. Fig. 2
164 shows the distance between track T165 and T31, ~7.5 km without considering ice flow. However
165 because of the fast moving ice tongue, the distance of their actual ground tracks on the surface of
166 the MIT should be a little larger because T165 is located upstream and observed later. Thus
167 footprints relocation using ice velocity is critical to obtain accurate geometric relations among
168 different tracks. The ice velocity data from Rignot et al. (2011) generated from InSAR data from
169 2006 to 2010 is used to relocate the footprints of ICESat/GLAS. Thus the correct geospatial
170 relations between observations from different campaigns can be achieved on November 14, 2002,
171 March 8, 2004, December 27, 2006, and January 31, 2008, through Eqs. (2) and (3). The
172 freeboard change with time should be considered as well, but this contribution is neglected
173 because freeboard comparison from crossing tracks showed a slightly decreasing trend of -0.06

174 m/a on average (Wang et al. 2014). The spatial distribution of freeboard data over the MIT
175 corresponding to November 14, 2002, is shown in Fig. 5(a).

176
$$X = x + \sum_{i=1}^n v_{xi} \Delta t + v_{xm} t_m \quad (2)$$

177
$$Y = y + \sum_{i=1}^n v_{yi} \Delta t + v_{ym} t_m \quad (t_m = t_2 - t_1 - n \Delta t) \quad (3)$$

178 where ‘x’ and ‘y’ is location in the X and Y directions from ICESat measurement directly;
179 ‘X’ and ‘Y’ is location in the X and Y directions after relocation; ‘v_x’ and ‘v_y’ is the ice velocity
180 in the X and Y directions respectively; ‘t₁’ and ‘t₂’ is the start and end time; ‘Δt’ is the time
181 interval and ‘n’ indicates the largest integer time steps for time interval between ‘t₁’ and ‘t₂’;
182 ‘t_m’ is the residual time; In this work, ‘Δt’ is set as 10 days; ‘v_{xi}’ and ‘v_{yi}’ is derived from ice
183 velocity field according to different locations during relocation and may change in different time
184 intervals.

185 The forth step ~~was is~~ to interpolate the freeboard map using the relocated freeboard data
186 from step three. with Inverse Distance Weighting, Natural Neighbor, Spline and Kriging are
187 most widely used interpolation techniques (Childs. 2004). a Kriging interpolation under spatial
188 analysis toolbox of ArcGIS is selected in this study to produce freeboard maps of the MIT
189 because kriging can provide an optimal interpolation estimate for a given coordinate location by
190 considering the spatial relationships of a data set. method. With this method, freeboard maps of
191 the MIT are produced on November 14, 2002, March 8, 2004, December 27, 2006, and January
192 31, 2008 ~~respectively,~~ because of known ice tongue outlines from Landsat images.

193 Ice draft is calculated with Eq. (24) assuming hydrostatic equilibrium and the lowest sea-
194 surface height (further discussed later in Section 6.2.2) is extracted as well from ICESat/GLAS
195 data from all campaigns covering this region, which was -3.35 m under EGM 08 (WGS-84). ~~In a~~
196 ~~background of changing tidal~~ For time varying sea-surface heights caused by tides, the minimum

Formatted: Font: Times New Roman, Not Italic

Formatted: Font: Times New Roman, Not Italic

Formatted: Font: Italic

Formatted: Font: Italic

Formatted: Font: Not Italic

Formatted: Font: Italic

Formatted: Font: Italic

197 ~~sea-sea~~-surface height can allow ice with a given draft to ~~most strongly~~ ground to the seafloor.
 198 Then, ice bottom elevation is calculated by considering the ice draft and the lowest sea-surface
 199 height. To compare the ice bottom with the seafloor, an elevation difference of both is calculated.
 200 In this way, a negative value indicates that ice bottom is lower than seafloor, which corresponds
 201 to ~~a~~-grounding ~~phenomenon~~.

$$202 \rho_w D = \rho_i (H_f + D - FAC) \quad (24)$$

203 where ‘ D ’ is ice draft, i.e. vertical distance from sea surface to bottom of ice; ‘ H_f ’ is freeboard,
 204 i.e. vertical distance from sea surface to top of snow; ‘ ρ_w ’ and ‘ ρ_i ’ are densities of ocean water
 205 and ice, respectively. In this study, ice and sea water density are taken as 915 kg/m^3 and 1024
 206 kg/m^3 , respectively (Wang et al., 2014); ‘ FAC ’ is the firm air content, the decrease in thickness
 207 (in meters) that occurs when the firm column is compressed to the density of glacier ice, ~~the same~~
 208 as ~~what was~~ defined in Holland et al., (2011) and Ligtenberg et al. (2014). The calculation of firm
 209 air content around Mertz will be soon introduced in Section 3.2. In this ~~paperwork~~, we define the
 210 elevation of at the underside (bottom) of the tongue as ‘ E_{ice_bottom} ’ and ~~it can be is~~ calculated by
 211 Eq. (35). ~~Similarly, the elevation difference of ice tongue bottom and seafloor is defined as~~
 212 ~~‘ E_{dif} ’, which can be calculated by Eq. (4).~~

$$213 E_{ice_bottom} = E_{sea_level} - D \quad (35)$$

214 where ‘ E_{ice_bottom} ’ corresponds to elevation of the ice bottom. ‘ E_{sea_level} ’ is the lowest ~~sea-sea-~~
 215 surface height among extracted sea-surface height from different tracks and different campaigns,
 216 which is -3.35 m. Similarly, the elevation difference of ice tongue bottom and seafloor is defined
 217 as ‘ E_{dif} ’, which can be calculated by Eq. (6).

$$218 E_{dif} = E_{ice_bottom} - E_{sf} \quad (46)$$

219 where ‘ E_{dif} ’ is elevation difference by subtracting the seafloor elevation from the ice bottom.

220 3.2. Firn Air Content Estimation Method

221 The Antarctic ice sheet is covered by a dry, thick firn layer, which represents an
222 intermediate stage between fresh snow and glacial ice, having a varying density between 350
223 km/m³ and 900 km/m³ from Antarctic inland to the coast (Van den Broke, 2008). The density of
224 firn layer increases from the surface to the bottom, which usually follows an exponential
225 distribution of depth (Patersen, 1994). Using a combination of regional climate model output and
226 steady state firn compaction model. The density and depth of the Antarctic firn layer has been
227 modeled (e.g., Van den Broke, 2008) using a combination of regional climate model output and a
228 steady-state firn compaction model). However, for ice thickness inversion, Firn Air Content
229 (FAC) is usually used to make the calculation convenient (Rignot and Jacobs, 2002), defined as
230 the decrease in thickness (in meters) that occurs when the firn column is compressed to the
231 density of glacier ice (Holland et al., 2011). Time-dependent Firn Air Content (FAC) was has
232 also been modeled by considering the physical process of the firn layer (e.g., Ligtenberg et al.
233 2014). For the MIT, there are some in-situ measurements of snow thickness available from
234 Massom et al. (2010) who used a snow layer depth of 1 m to derive the thickness of surrounding
235 multi-year, fast sea ice. However on the surface of the MIT, no in-situ measurements of density
236 and or depth of firn layer are available.

237 Because of different density and thickness of the firn layer on top layer of an ice tongue,
238 it is challenging to simulate the density profile of the MIT without in-situ measurements as
239 control points. In this study, we use FAC extracted from adjacent seafloor-touching icebergs to
240 investigate the grounding of the MIT rather than FAC from modeling. MIT may be composed of
241 pure ice, water, air, firn or snow that makes ice mass calculation complicated. However, if
242 assuming a pure ice density only to calculate ice mass, the thickness of MIT must be corrected

243 by FAC. FAC correction to ice thickness can be inferred from surrounding icebergs calving from
244 MIT using Eq. (4) when knowing ice draft and freeboard assuming hydrostatic equilibrium.
245 Thus one critical issue is to target and use icebergs fulfilling these requirements to solve Eq. (4),
246 such as slightly grounded icebergs above already known seafloor with observed freeboard.

247
248 ~~To invert glacial ice thickness from freeboard observation under hydrostatic assumption,~~
249 ~~one can use a two-layer density model, which consists of an upper firn layer and a lower glacial~~
250 ~~layer (Luckman et al., 2010). In the upper layer, firn density varies with depth. However, in the~~
251 ~~lower glacial layer, the density is considered a constant. One can also use FAC to correct the~~
252 ~~inversed ice thickness assuming hydrostatic equilibrium (Rignot and Jacobs, 2002). In this study,~~
253 ~~we use FAC extracted from adjacent seafloor touching icebergs to investigate the grounding of~~
254 ~~the MIT rather than FAC from modeling.~~

255 From Smith (2011), icebergs can be divided into three categories based on topography
256 bathymetry and seasonal pack ice distributions: grounded ~~iceberg~~, constrained ~~iceberg~~, and free-
257 drifting icebergs. Without occurrence of pack ice, an iceberg can be free-drifting or grounded.
258 Free-drifting icebergs can move several tens of kilometers per day, such as iceberg A-52 (Smith
259 et al. 2007). Grounded icebergs can be firmly or lightly anchored. Heavily grounded icebergs
260 have firm contact with the seafloor and can be stationary for a long time, such as iceberg B-9B
261 (Massom. 2003). However, slightly grounded icebergs may have little contact with the seafloor
262 and can possibly move slowly under the influence of ocean tide, ocean currents, or winds, but
263 much slower than free-drifting icebergs. The relation of grounding-grounded and ice drifting
264 velocity is not well-known. However, from slowly drifting or nearly stationary icebergs in open
265 water, we can determine if an iceberg is grounded.

266 Because of the heavily grounded iceberg B-9B to the east of the MIT blocking the
267 drifting of pack ice or icebergs from the east, icebergs located between B-9B and the MIT are
268 most likely generated from the Mertz or Ninnis glaciers. We ~~can~~ calculate the FAC from these
269 icebergs and later apply it to grounding event detection of the MIT, in terms of estimating the
270 FAC of the MIT itself. Around the MIT, the locations of three icebergs ('A', 'B' and 'C') were
271 identified using MODIS and Landsat images in austral summer, 2006 and 2008 and shown in Fig.
272 64. Fortunately, ICESat/GLAS observed these icebergs on February 23, 2006 (54th day of 2006)
273 and February 18, 2008 (49th day of 2008). ~~These~~ This allows us to analyze the behavior of the
274 icebergs three-dimensionally. From Fig. 4a, icebergs 'A', 'B' and 'C' changed position little in
275 about two months (from 28 to 85 day of 2006). Thus we can consider these icebergs slightly
276 grounded. These slightly grounded icebergs may plough the seafloor and leave ridges or grooves.
277 In Pine Island Trough, ridges on the seafloor have been already found with a range of 1 to 2 m,
278 which was believed to be influenced by grounding icebergs drifting with tides (Jakobsson et al.
279 2011; Woodworth-Lynas et al. 1991). From this viewpoint, we are confident that under the
280 lowest sea level (lowest tide), these iceberg must be grounded, which means that the ice draft
281 ~~inversed-inverted~~ from freeboard measurement assuming hydrostatic equilibrium must be greater
282 than or equal to water depth. Based on this analysis, we can take water depth as draft to
283 calculate the FAC ~~and the FAC calculated with this method should be less than or equal to the~~
284 ~~absolute value.~~

285 Because only 'A' and 'C' were observed by track T1289 of the ICESat/GLAS in 2006,
286 freeboard and water depth from bathymetry for both are used to calculate the FAC (Fig. 4, 9 and
287 Table 1). However, the icebergs were not stationary, which indicates only some parts were
288 grounded. In this study, only the top two largest ~~measurements of each~~ freeboard measurements

289 of icebergs 'A' and 'C' from profile T1289 in 2006 are employed to calculate the FAC with Eq.
290 (27) with a least-least-squares method under hydrostatic equilibrium. The result is listed in Table
291 1.

$$292 \quad FAC = H_{f_k} + D_k - \frac{\rho_w}{\rho_i} D_k + \varepsilon_k \quad (7)$$

293 where 'k' is used to identify different icebergs 'A' or 'C', 'H_f' is the top two largest freeboard
294 measurement of each iceberg, 'D' is ice draft which is the same as sea water depth and is taken
295 from seafloor bathymetry directly, 'ε' is a residual for FAC.

296 From Table 1, we can find the average Table 1 shows the freeboard and seafloor
297 bathymetry under the icebergs in 2006 for FAC calculation and grounding detection of icebergs
298 in 2008 (detailed freeboard values for these icebergs can be seen from Fig. 9). With freeboard
299 and seafloor measurements from iceberg 'A' and 'C' in 2006 (Table 1), the FAC is calculated as
300 about 4.87 ± 1.31 m. Under this FAC setting, the accuracy of grounding detection with this
301 method is about ± 11 m (one standard deviation of the residuals). Two icebergs 'A' and 'B' were
302 observed by the same track T1289 of the ICESat/GLAS on February 18, 2008 and thus are used
303 to evaluate the grounding detection using this FAC result. From positions-iceberg trajectories
304 observed by remote sensing in (Fig. 4b), we know, iceberg 'A' drifted away from its original
305 position. Thus it was not grounded. However, iceberg 'B' kept rotating in this period without
306 drifting away, from which we can consider it grounded. Such grounding status determined from
307 remote sensing can also be detected with our method since the elevation difference of ice
308 bottom and seafloor is shown in from Table 1, from which we can see that does clearly indicate a
309 grounding-grounded iceberg 'B' and a floating iceberg 'A' is clearly identified. Thus, our the
310 FAC estimation works well around Mertz.

Formatted: Indent: First line: 0"

Formatted: Font: Italic

Formatted: Font: Italic

311 ~~Actually, for FAC calculation, icebergs just touching the seafloor should be used, in~~
 312 ~~which case, the FAC calculated assuming hydrostatic equilibrium is the same as the actual value.~~
 313 ~~However, it is difficult to ascertain whether an iceberg is just touching the seafloor from remote~~
 314 ~~sensing images. The near stationary or slowly rotating iceberg detected should be grounded more~~
 315 ~~severely than one just touching the seafloor, which results in a calculated FAC theoretically~~
 316 ~~larger than the actual value. Thus using this FAC result to detect grounding can lead to smaller~~
 317 ~~grounding results. However, once an iceberg or ice tongue is detected as grounded, the result~~
 318 ~~should be robust.~~

319 **4. Accuracy ~~Prediction for of~~ Grounding Detection**

320 The accuracy of ‘ E_{dif} ’ is critical to grounding detection of the MIT. From Eq. (1) to (46),
 321 we ~~can~~ find different components of the error sources, such as ~~errors~~ from sea surface height
 322 determination, ice draft, seafloor bathymetry, and elevation transformation. Meanwhile,
 323 uncertainty of ice draft is primarily determined by that of freeboard and ‘FAC’. Furthermore, the
 324 uncertainty of freeboard is influenced by footprint relocation and freeboard changing rates.
 325 Considering all mentioned above, the error source of elevation difference ‘ E_{dif} ’ can be
 326 synthesized by Eq. (58):

$$327 \Delta E_{dif} = \Delta E_{sl} + a(\Delta H_f + \Delta E_{re} + \Delta E_{fb_c} + \Delta FAC + \Delta E_{krig}) + \Delta E_{sf} + \Delta E_{trans} \quad (58)$$

328 where $a = \frac{\rho_i}{\rho_w - \rho_i}$; ‘ Δ ’ stands for error of each variable; ‘ ΔE_{dif} ’ stands for error of final elevation
 329 difference of ice bottom and seafloor; ‘ ΔE_{sl} ’, ‘ ΔH_f ’, ‘ ΔE_{re} ’, ‘ ΔE_{fb_c} ’, ‘ ΔFAC ’, ‘ ΔE_{sf} ’ and
 330 ‘ ~~ΔE_{krig}~~ ’, ‘ ΔE_{trans} ’ stand for errors caused by sea surface height extraction, freeboard extraction,
 331 freeboard relocation, freeboard changing rates, FAC calculation, seafloor bathymetry, kriging
 332 interpolation and elevation system transformation, respectively.

333 Usually, the influence of elevation system transformation on final elevation difference
334 can be neglected. Based on the error propagation law, the uncertainty of elevation difference
335 ‘ E_{dif} ’ can be described by Eq. (69):

$$\varepsilon E_{dif} = \sqrt{(\varepsilon E_{sl})^2 + a^2[(\varepsilon H_f)^2 + (\varepsilon E_{re})^2 + (\varepsilon E_{fb_c})^2 + (\varepsilon FAC)^2 + (\varepsilon E_{krig})^2] + (\varepsilon E_{sf})^2}$$

337 (69)

338 where ‘ ε ’ indicates the uncertainty of each parameter.

339 **4.1 Uncertainty of kriging interpolation**

340 Fig. 5a shows the spatial distribution of freeboard data over the MIT used for detecting
341 grounding on November 14, 2002. The spatial difference of ICESat/GLAS between Fig. 2 and
342 Fig. 5 are caused by footprint relocation, after which the spatial geometry between different
343 tracks is relatively correct. In the lower right of the Mertz ice front (Fig. 5a), the freeboard
344 distance between track T1289 and T165 is about 7 km. In these data gaps, freeboard data used
345 for grounding detection in Section 3.1 is interpolated using kriging. Thus, knowing the
346 uncertainty of kriging interpolation is critical to final grounding detection.

347 To investigate interpolation uncertainty of the kriging method, freeboard measurements
348 should be compared with interpolation ones. Thus, a testing region with freeboard measurements
349 is selected, indicated by a blue dashed square in Fig. 5a, about 7 km×7 km. A freeboard map is
350 first interpolated with gray dots only (Fig. 5a) using kriging. Then, the freeboard measurements
351 (284 of green dots in Fig. 5a) are compared with interpolation in the square. The spatial
352 distribution and the histogram of freeboard difference derived by subtracting krigged freeboard
353 from freeboard derived from ICESat/GLAS is shown in Fig. 5b.

Formatted: Font: Bold

Formatted: Font: Bold

Formatted: SM Text, Indent: First line: 0.5"

354 In this square, the freeboard measurement varies from 31.6 m to 40.0 m with 36.6 m as
355 the average. However, the freeboard interpolation varies from 32.9 m to 39.6 m with 35.9 m as
356 the average. From the freeboard difference results (Fig. 5b), we find that the interpolation results
357 show similar results compared with freeboard derived from ICESat/GLAS. The interpolated
358 freeboard has an accuracy of -0.7 ± 1.8 m. The interpolated freeboard using kriging can reflect
359 the actual freeboard well. Also, the distribution of freeboard difference in Fig. 5b does not show
360 obvious geospatial variation trend.

361 4.2 Grounding Detection Robustness

362 Since sea level is extracted from ICESat/GLAS data track by track, we use ± 0.15 m as
363 the uncertainty of elevation data (ϵE_{sl}). Also from Wang et al. (2014), we can see the
364 uncertainty of freeboard extraction (ϵH_f) is ± 0.50 m. From Rignot et al. (2011), the error of ice
365 velocity ~~here~~ ranged from 5 m/a to 17 m/a. Assuming that ice velocity varied by 17 m/a (an
366 upper threshold), the relocation error horizontally could reach ± 54 m in an average of three years²
367 ~~time~~. Wang et al. (2014) extracted the average slope of the MIT along ice flow direction as
368 0.00024. However, because of large crevasses on the surface, we use 50 times of this value as an
369 conservative estimate of the average slope. In this way, we can estimate ' ϵE_{re} ' as ± 0.65 m when
370 considering a three-year period. The annual rate of freeboard change ~~annual changing rate of~~
371 ~~freeboard~~ from 2003 to 2009 is -0.06 m/a (Wang et al. 2014). Therefore, we consider the
372 freeboard stable ~~in~~ over this period. However, when combining data from different time periods
373 then ' ϵE_{fb_c} ' is estimated as about ± 0.18 m if considering three years² time difference. From
374 Beaman et al. (2011), considering elevation uncertainty at the worst situation when water depth
375 is 500 m, ' ϵE_{g104c} ' is ± 11.5 m. For kriging interpolation, from analysis in Section 4.1, 1.8 m is

Formatted: Font: Bold

Formatted: SM Text

Formatted: Font: Bold

376 ~~taken as the uncertainty.~~ Using all these errors above, we calculate the final uncertainty of
377 elevation difference as $\pm 17\text{-}23$ m.

378 From the calculations above, we can say that ' E_{dif} ' less than $-17\text{-}23$ m corresponds to a
379 very robust grounding event. However, if the ' E_{dif} ' is greater than $17\text{-}23$ m, we can not confirm
380 ~~no grounding there.~~ ' E_{dif} ' in the interval of $-17\text{-}23$ m to $17\text{-}23$ m corresponds to slight
381 grounding or floating. We can also determine different contributions of each separate factor to
382 the overall accuracy. Seafloor bathymetry contributes the largest part and is the dominant factor
383 affecting the accuracy of grounding detection.

384 5. Grounding Detection Results

385 The spatial distribution of elevation difference ' E_{dif} ' and outline of the MIT from 2002
386 to 2008 ~~can be found~~ is shown in Fig. 56. A buffer region with ~~buffer~~ radius of 2 km (region
387 between black and grey lines in Fig. 56) is ~~also~~ introduced to investigate grounding potential of
388 the MIT, if it approached there. The elevation difference less than $34\text{-}46$ m (twice of elevation
389 difference uncertainty ' εE_{dif} ') both inside and outside of the outline is extracted and the
390 corresponding statistics are shown in Table 2. Since the uncertainty to determine a grounding
391 event is about $\pm 17\text{-}23$ m, if some grid points of the MIT have elevation difference ' E_{dif} ' less
392 than $17\text{-}23$ m, we can conclude that this section of the tongue is almost grounded. The smaller
393 the ' E_{dif} ', the more robust the grounding. From the color-change patterns of Fig. 5a6a-d, we can
394 see that part of the ice front grounded on the shallow Mertz Bank from the end of 2002.

395 As illustrated from Table 2, the minimum ' E_{dif} ' inside of the MIT are all less than $17\text{-}23$
396 m and the mean and minimum of the ' E_{dif} ' in the buffer region are all less than 0 from 2002 to
397 2008. From this, we ~~can~~ conclude that the ice tongue has grounded on the shallow Mertz Bank
398 since November 14, 2002. This result coincides with findings from Massom et al. (2015) who

399 considered that the northwestern extremity of the MIT started to contact with the seafloor shoal
400 in late 2002 to early 2003. Also it would be hard for the MIT to approach the buffer region
401 (indicated with yellow to red color in Fig. 56) as the surrounding Mertz Bank gets shallower and
402 steeper and substantive grounding would happen if it moved into these regions. Inside of the
403 MIT, the minimum of elevation difference was just 11.9 m on November 14, 2002, which
404 indicates little to no grounding. However on March 8, 2004, December 27, 2006, and January 31,
405 2008, the minimum of elevation difference reached -46.0 m, -52.3 m and -34.8m respectively,
406 which means significant grounding occurred in some regions. From 2002 to 2008, more regions
407 under the MIT have 'E_{dif}' less than 46 m, the area of which increased from 8 km² to 17 km².
408 Additionally, the mean of 'E_{dif}' ~~inside-under~~ of the tongue for those having 'E_{dif}' less than 46
409 m gradually decreases from ~~25.0~~28.8 m to 12.3-0.8m, according to which we can conclude that
410 the ice front was grounded more significantly with passing time. Additionally, since the
411 grounding area increased from ~~6-8~~ km² to ~~13-17~~ km² (Table 2) and the mean of 'E_{dif}' decreased
412 from 2002 to 2008, we can say that over the period from 2002 to 2008, the grounding of the
413 northwest flank of the MIT became more widespread.

414 Based on the calculated elevation difference, the grounding outlines of the MIT are
415 delineated ~~on-for~~ November 14, 2002, March 8, 2004, December 27, 2006 and January 31, 2008,
416 ~~respectively~~ (Fig. 67). For the grounding part of the outline in different years, starting and ending
417 location and perimeter are also extracted, from which we can conclude that the length of the
418 grounding outline ~~because~~ of the Mertz Bank is only limited to a few kilometers (Table 3).

419 We find that the lower right (northwest) of the MIT was always grounded and that-
420 ~~However,~~ grounding did not occur in other regions (Fig. 56). The shallowest seafloor elevation
421 the ice front touched was ~ -290 m in November 2002. In 2004, 2006, and 2008, the lower right

Formatted: Superscript

Formatted: Superscript

422 | (northwest) of the MIT even approached the contour of -220 m. Fig. ~~6-7~~ also shows the
423 | extension line of west flank in November, 2002, from which we can see that if the ice tongue
424 | moved along the former direction, the ice flow would be seriously blocked when approaching the
425 | Mertz Bank. The shallowest region of the Mertz Bank ~~ahead~~ has an elevation of about -140 m
426 | and the MIT would have needed to climb over thus 140 m obstacle to cross past it. The shallow
427 | Mertz Bank would have caused grounding during the climbing. This special feature of seafloor
428 | shoal facing the MIT can further explain why the ice velocity differed along the east and west
429 | flanks of the MIT before calving and why the ice tongue moved clockwise to the east, as pointed
430 | out by Massom et al. (2015). However, because of sparsely-distributed bathymetry data (point
431 | measurements) in Mertz region used in Massom et al. (2015), this effect could not be easily seen.
432 | Here, from our grounding detection results and surrounding high-accuracy bathymetry data, this
433 | effect is more clearly observed.

434 | **6. Discussion**

435 | **6.1 Area Changing Rate and ~70-year Calving Cycle of MIT**

436 | Using Landsat TM/ETM+ images from 1989 to 2013, outlines of the MIT are extracted
437 | manually. Assuming a fixed grounding line position over this period, the area of the MIT over
438 | this period is calculated. Using these data, from 1989 to 2007, an ~~area-increasing~~ area rate~~trend~~
439 | of the MIT is shown (from 5453 km² to 6126 km²) in Fig. ~~78~~. However, the area of the MIT was
440 | almost constant from 2007 to 2010, before calving. The largest area of the MIT was 6113 km²
441 | closest to the calving event in 2010. After the calving, the area decreased to 3617 km² in
442 | November 2010.

443 | The ~~rate of~~ area change~~-expanding trend~~ for the MIT from 1989 to 2007 is also obtained
444 | using a least-squares method, ~~giving a value of~~corresponding to 35.3 km²/a. However, after the

445 calving a slight higher area-increasing trend of $36.9 \text{ km}^2/\text{a}$, is found (Fig. 7). On average, the
446 area-increasing rate of the MIT was $36 \text{ km}^2/\text{a}$.

447 The surface behavior such as ice flow direction changes and middle rift changes caused
448 by grounding was analyzed by Massom et al. (2015). In the history of the MIT, one or two large
449 calving events were suspected to have happened between 1912 and 1956 (Frezzotti et al., 1998)
450 and we consider it likely to be only once because of the influence of the shallow Mertz Bank.
451 When the ice tongue touched the bank, the bank started to affect the stability of the tongue by
452 bending the ice tongue clockwise to the east, as can be seen from velocity changes from Massom
453 et al. (2015). With continuous momentum and flux input from upstream, a large rift from the
454 west flank of the tongue would ultimately have to occur and could potentially calve the tongue.
455 A sudden length shortening of the tongue can be caused by such ice tongue calving as indeed had
456 happened in February, 2010. We also consider that even without a sudden collision of iceberg B-
457 9B in 2010, the ice tongue would eventually calve because of existence of the shallow Mertz
458 Bank.

459 If we take 6127 km^2 as the maximum area of the MIT, assuming a constant area-changing
460 rate of about $36.9 \text{ km}^2/\text{a}$ after 2010, it will take about 68 years to calve again. When assuming an
461 area changing rate of about $35.3 \text{ km}^2/\text{a}$ as before 2010, it will take a little longer, about 71 years.
462 Therefore, without considering accidental event such as collision with other large icebergs, the
463 MIT is predicted to calve again in ~ 70 years. Because of the continuous ice flow upstream, the
464 special location and relatively lower depth of the Mertz Bank, the calving is likely repeatable and
465 a cycle therefore ~~does~~ exists.

466 After the MIT calved in February, 2010, Mertz polynya size, ~~sea-sea~~-ice production, sea-
467 ice coverage and high-salinity shelf water formation changed. A ~~sea-sea~~-ice production decrease

468 of about 14-20% was found by Tamura et al. (2012) using satellite data and high-salinity shelf
469 water export was reported to reduce up to 23% using a state-of-the-art ice-ocean model
470 (Kusahara et al. 2010). Recently, Campagne et al. (2015) pointed out a ~70-year cycle of surface
471 ocean condition and high-salinity shelf water production around Mertz through analyzing
472 reconstructed sea ice and ocean data over the last 250 years. They also mentioned that this cycle
473 was closely related to presence and activity of Mertz polynya. However, the reason for this cycle
474 was not fully understood.

475 From these findings addressed above and MIT calving cycle we found, our explanation is
476 that the calving cycle of the MIT leads to the ~70-year cycle of surface ocean condition and
477 high-salinity shelf water production around Mertz. Calving decreases the length of the MIT
478 suddenly. Then, Aa short ice tongue reduces the size of Mertz Polynya formed by Antarctic
479 katabatic winds ~~and, results resulting~~ in lower ~~sea-sea~~ ice production and further lessens high-
480 salinity shelf water production. Therefore, the cycle of ocean conditions around Mertz found by
481 Campagne et al. (2015) is likely dominated by the calving of the MIT. Additionally, the cycles of
482 MIT calving and surface ocean condition around Mertz coincides with each other well, ~70 years,
483 which make the explanation much ~~exact~~ more compelling.

484 **6.2 Key issues influencing grounding detection**

Formatted: Font: Bold

485 Several issues on grounding detection require further clarification, such as sea surface
486 height, FAC value and accuracy of seafloor DEM. In this section, their influences on final
487 grounding detection results are more deeply discussed.

Formatted: Indent: First line: 0.5"

488 **6.2.1 The Lowest Sea-Level Extraction**

Formatted: Font: Bold

489 In Section 3.1, the lowest sea level -3.35 m is derived by comparing all sea-surface
490 heights derived from different tracks and campaigns from 2003 to 2009. This constant stands for

Formatted: Indent: First line: 0.5"

491 the lowest sea level from results around Mertz from 2003 to 2009 and is directly from
492 ICESat/GLAS observation. However, because of limited observations in each year,
493 ICESat/GLAS may not catch the lowest one. Sea level lower than -3.35 m may exist over Mertz
494 region which would make the grounding results more severe with occurrence of more negative
495 values in Fig. 6.

496 **6.2.2 Firn Air Content Calculation**

Formatted: Font: Bold

497 FAC varies across the Antarctica ice sheet, usually decreasing from the interior to the
498 coast. In Section 3.2, FAC over Mertz region is derived as 4.87±1.31 m. However from time-
499 dependent FAC modeling results, around Mertz region, FAC is closed to 5-10 meter (Ligtenberg
500 et al. 2014). Our result is smaller. Since there are no in-situ measurements available for
501 verification, further comparison work needs to be conducted. However, this FAC value is
502 derived according to our best knowledge over Mertz and is affected by iceberg status (using our
503 approach) and the maximum freeboard used.

Formatted: Indent: First line: 0.5"

504 First, for FAC calculation, icebergs just touching the seafloor should be used in which
505 case the FAC calculated assuming hydrostatic equilibrium is the same as the actual value.
506 However, it is difficult to ascertain whether an iceberg is just touching the seafloor from remote
507 sensing images. The near stationary or slowly rotating iceberg detected with remote sensing
508 should be grounded more severely than just touching the seafloor, which may result in a
509 calculated FAC theoretically larger than the actual value. Thus, using this FAC result to detect
510 grounding can potentially lead to smaller grounding results. However, once an iceberg or ice
511 tongue is detected as grounded, the result is more convincing.

512 Second, because ICESat/GLAS worked only several times a year on repeat tracks and
513 icebergs was rotating slowly, elevation profile in 2006 and 2008 along the same track T1289

514 may not come from the same ground surface. Fig. 9 shows the freeboard over iceberg ‘A’, ‘B’
515 and ‘C’ derived from ICESat/GLAS from 2006 and 2008. By comparing freeboard of iceberg ‘A’
516 in 2006 (Fig. 9a), and 2008 (Fig. 9c), we can find that the maximum freeboard was larger and the
517 freeboard profile was longer in 2006. Comparatively, the smaller freeboard in 2008 may be
518 caused by ice basal melting or observing different portion of iceberg ‘A’. Since larger freeboard
519 measured in 2006 indicating a high possibility of capturing the thickest portion, the freeboard
520 measurement in 2006 is used to invert the FAC. Additionally, iceberg ‘A’ and ‘C’ did show the
521 similar maximum freeboard (Table 1), which is another important reason for us to choose
522 measurement in 2006 to invert.

523 **6.2.3 Seafloor DEM**

524 High accuracy seafloor elevation is critical to final success of grounding detection. As
525 can be seen from S-Fig.1, there is no bathymetry data under the MIT, which may result in large
526 uncertainty for seafloor interpolation. The oldest bathymetry data collected along margin of the
527 MIT was at least from 2000 (Beaman et al. 2011). Thus, the boundary of the MIT in 2000 is used
528 to identify bathymetry measurement gaps, as is indicated in Fig. 6. But around the Mertz Ice
529 front, both east and west flanks, bathymetry data does exist, which provides control points for
530 seafloor interpolation under the tongue. Since the ice front has a width of ~34 km (Wang et al.
531 2014), the accuracy of seafloor DEM under the MIT varies according to different distances to the
532 control points. Inside of the MIT boundary of 2000, the closer to the white polygon, the better
533 the accuracy the seafloor DEM. Outside of that boundary, the quality of the seafloor DEM data is
534 much better because of the high density of single-beam or multi-beam bathymetry measurements.

535 However, from Beaman et al. (2011), no uncertainty on the seafloor DEM was
536 systematically provided, but only the poorest accuracy of single or multi-beam bathymetric

Formatted: Font: Bold

Formatted: Indent: First line: 0.5"

537 measurements. Since no new bathymetry data is publicly available in this region, further work on
538 evaluation of the seafloor bathymetry is not possible to conduct and interpolation error from
539 kriging using bathymetry data is difficult to supply. Thus, the accuracy under poorest situation
540 for bathymetry data is used, the same as used in Beaman et al. (2011).

541 Since Beaman et al. (2011) provided the most accurate seafloor DEM over Mertz
542 according to our best knowledge, seafloor DEM under the MIT is kept and the grounding
543 detection is conducted as well. Additionally, the ice tongue never stopped flowing further into
544 the ocean, where the bathymetry measurements density is good. From results shown in Fig. 6 all
545 grounding sections of MIT boundary are located outside of the 2000 boundary. Thus the analysis
546 of grounding detection near ice front in 2002, 2004, 2006, and 2008 is convincing. Inside of the
547 2000 boundary, most of the grounding detection results are above 100 m, indicating a floating
548 status of the corresponding ice. Only abnormal seafloor features higher than this seafloor DEM
549 by about 100 m can result in wide grounding inside. Additionally, from surface features of the
550 MIT from Landsat TM/ETM+ images, no abrupt sunlight shadow related to grounding is
551 detected from 1989 to 2010 near the front, which indicates that the judgment of floating ice
552 tongue inside of the 2000 boundary from Fig. 6 is correct. Actually, no matter whether the MIT
553 inside of the 2000 boundary was grounded or not, gradually grounding on the shallow Mertz
554 Bank of the MIT since late 2002 is a fact, which is direct evidence for us to infer the primary
555 cause of the instability of the MIT.

556 **6.2 Iceberg Scouring Detection**

557 ~~Icebergs play an important role in sediment transport and distribution. Also grounded~~
558 ~~iceberg can scour the seafloor and disturb the benthic communities on parts of the Antarctic~~
559 ~~continental shelf. Iceberg scouring across the George V shelf was detected by Post et al. (2011).~~

560 ~~A recent marine science voyage to the Mertz glacier region was conducted onboard the~~
561 ~~Australian Antarctic research vessel Aurora Australis in 2011 and one objective of this voyage~~
562 ~~was to investigate benthic community composition in iceberg scours (Smith and Riddle, 2011).~~
563 ~~A camera station was set around the Mertz Bank in an attempt to detect iceberg scours caused by~~
564 ~~the MIT. However, the photos collected from this station indicated no scours. The grounding of~~
565 ~~the Mertz ice front on the Mertz Bank can leave scours but the camera station was far from~~
566 ~~grounding regions of the ice tongue by several kilometers. Since the tongue did not move across~~
567 ~~that place, it is unlikely to find recent scours. We suggest possible new scours detection along the~~
568 ~~margin of the grounding ice tongue as indicated with thick lines in Fig. 6.~~

569 **7. Conclusion**

570 In this study, a method of FAC calculation from seafloor-touching icebergs around Mertz
571 region ~~was is~~ presented as an important element of understanding MIT grounding. The FAC
572 around the Mertz is about 4.87 ± 1.31 m. This FAC is used to calculate ice draft based on sea level
573 and freeboard extracted from ICESat/GLAS and appears to work well. A method to extract
574 grounding sections of the MIT ~~was is~~ described based on comparing ~~inverted~~ ice draft assuming
575 hydrostatic equilibrium with seafloor bathymetry. The final grounding results explain the surface
576 behavior of the MIT. Previous work by Massom et al. (2015) has also provided some evidence
577 for seafloor interaction, in showing that the MIT front had an approximate 280 m draft with the
578 nearby seafloor as shallow as 285 m, suggesting the possibility of grounding. In our work, we
579 have provided ample detailed bathymetry and ice draft calculations. Specifically, ice bottom
580 elevation ~~was is~~ ~~inversed~~ inverted using ICESat/GLAS data and compared with seafloor
581 bathymetry during 2002, 2004, 2006, and 2008. From those calculations we show conclusively
582 that the MIT was indeed grounded along a specific portion of its northwest flank over a limited

583 | region. We also pointed out that even without collision by iceberg B-9B in early 2010 the ice
584 | tongue would eventually have calved because of momentum and flux input from the upstream
585 | glacier flow being increasingly opposed by a reaction force from the shoal of the Mertz Bank.

586 | From remote sensing images we ~~were~~are able to quantify the rate of increase of area of
587 | the MIT before and after the 2010 calving. While the area-increasing trend of the MIT after
588 | calving is slightly larger than before, we used the averaged rate to estimate a timescale required
589 | for the MIT to re-advance to the area of the shoaling bathymetry from its retreated, calved
590 | position. Our estimate is ~70-years, which is remarkably consistent with Campagne et al. (2015)
591 | who found a similar period of sea surface changes using seafloor sediment data. A novel point
592 | we bring out in our study is that it is the shoaling of the seafloor combined with the rate of
593 | advance of the MIT that leads to the 70-year repeat cycle. Also the calving cycle of the MIT
594 | explains the observed cycle of sea surface conditions change well, which indicates the calving of
595 | the MIT is dominant factor for ~~sea~~sea-surface condition change. Understanding the mechanism
596 | underlying the periodicity of MIT calving is important as the presence or absence of the MIT has
597 | a profound impact on sea ice and hence of bottom water formation in the local region.

598 | **Acknowledgements**

599 | This research was supported by Fundamental Research Fund for the Central University,
600 | the Center for Global Sea Level Change (CSLC) of NYU Abu Dhabi (Grant-~~no~~: G1204), the
601 | Open Fund of State Key Laboratory of Remote Sensing Science (Grant-~~no~~: OFSLRSS201414),
602 | and the China Postdoctoral Science Foundation (Grant-~~no~~: 2012M520185, 2013T60077). We are
603 | grateful to the Chinese Arctic and Antarctic Administration, the European Space Agency for free
604 | data supply under project C1F.18243, the National Snow and Ice Data Center (NSIDC) for the
605 | availability of the ICESat/GLAS data (<http://nsidc.org/data/order/icesat-glas-subsetter>) and

606 MODIS image archive over the Mertz glacier ([http://nsidc.org/cgi-](http://nsidc.org/cgi-bin/modis_iceshelf_archive.pl)
607 [bin/modis_iceshelf_archive.pl](http://nsidc.org/cgi-bin/modis_iceshelf_archive.pl)), British Antarctica Survey for providing Bedmap-2 seafloor
608 topography data (<https://secure.antarctica.ac.uk/data/bedmap2/>), the National Geospatial-
609 Intelligence Agency for publicly released EGM2008 GIS data ([http://earth-](http://earth-info.nga.mil/GandG/wgs84/gravitymod/egm2008/egm08_gis.html)
610 [info.nga.mil/GandG/wgs84/gravitymod/egm2008/egm08_gis.html](http://earth-info.nga.mil/GandG/wgs84/gravitymod/egm2008/egm08_gis.html)), and the USGS for Landsat
611 data (<http://glovis.usgs.gov/>). ~~Also fruitful~~ discussions with M. Depoorter, P. Morin, T.
612 Scambos and R. Warner, and constructive suggestions from Editor Andreas Vieli and two
613 anonymous reviewers are acknowledged.

614 **References**

- 615 1. Beaman, R. J., & Harris, P. T. (2003). Seafloor morphology and acoustic facies of the
616 George V Land shelf. *Deep Sea Research Part II: Topical Studies in Oceanography*,
617 50(8), 1343-1355.
- 618 2. Beaman, R. J., O'Brien, P. E., Post, A. L., & De Santis, L. (2011). A new high-resolution
619 bathymetry model for the Terre Adélie and George V continental margin, East Antarctica.
620 *Antarctic Science*, 23(01), 95-103.
- 621 3. Berthier, E., Raup, B., & Scambos, T. (2003). New velocity map and mass-balance
622 estimate of Mertz Glacier, East Antarctica, derived from Landsat sequential imagery.
623 *Journal of Glaciology*, 49(167), 503-511.
- 624 4. Ballantyne, J., 2002. A multidecadal study of the number of Antarctic icebergs using
625 scatterometer data. Brigham Young University online report:
626 <http://www.scp.byu.edu/data/iceberg/IcebergReport.pdf> .

- 627 5. Campagne, P., Crosta, X., Houssais, M. N., Swingedouw, D., Schmidt, S., Martin, A., ...
628 & Massé G. (2015). Glacial ice and atmospheric forcing on the Mertz Glacier Polynya
629 over the past 250 years. *Nature Communications*, 6.
- 630 [6. Childs, C. \(2004\). Interpolating surfaces in ArcGIS spatial analyst. ArcUser, July-](#)
631 [September, 3235.](#)
- 632 ~~6,7~~ Depoorter, M. A., Bamber, J. L., Griggs, J. A., Lenaerts, J. T. M., Ligtnerberg, S. R. M.,
633 van den Broeke, M. R., & Moholdt, G. (2013). Calving fluxes and basal melt rates of
634 Antarctic ice shelves. *Nature*, 502(7469), 89-92.
- 635 ~~7,8~~ Domack, E., Duran, D., Leventer, A., Ishman, S., Doane, S., McCallum, S., ... & Prentice,
636 M. (2005). Stability of the Larsen B ice shelf on the Antarctic Peninsula during the
637 Holocene epoch. *Nature*, 436(7051), 681-685.
- 638 ~~8,9~~ Fretwell, P., Pritchard, H. D., Vaughan, D. G., Bamber, J. L., Barrand, N. E., Bell, R., ...
639 & Fujita, S. (2013). Bedmap2: improved ice bed, surface and thickness datasets for
640 Antarctica. *Cryosphere*, 7(1).
- 641 ~~9,10~~ Frezzotti, M., Cimbelli, A., & Ferrigno, J. G. (1998). Ice-front change and iceberg
642 behaviour along Oates and George V Coasts, Antarctica, 1912-96. *Annals of Glaciology*,
643 27, 643-650.
- 644 ~~10,11~~ Fricker, H. A., Young, N. W., Allison, I., & Coleman, R. (2002). Iceberg calving
645 from the Amery ice shelf, East Antarctica. *Annals of Glaciology*, 34(1), 241-246.
- 646 [12](#) Griggs, J. A., & Bamber, J. L. (2011). Antarctic ice-shelf thickness from satellite radar
647 altimetry. *Journal of Glaciology*, 57(203), 485-498.

- 648 | ~~11~~13. [Holland, P. R., Corr, H. F., Pritchard, H. D., Vaughan, D. G., Arthern, R. J.,](#)
649 | [Jenkins, A., & Tedesco, M. \(2011\). The air content of Larsen ice shelf. *Geophysical*](#)
650 | [Research Letters](#), 38(10).
- 651 | ~~12~~14. [Jakobsson, M., Anderson, J. B., Nitsche, F. O., Dowdeswell, J. A., Gyllencreutz,](#)
652 | [R., Kirchner, N., ... & Majewski, W. \(2011\). Geological record of ice shelf break-up and](#)
653 | [grounding line retreat, Pine Island Bay, West Antarctica. *Geology*, 39\(7\), 691-694.](#)
- 654 | ~~13~~15. [Jenkins, A., Dutrieux, P., Jacobs, S. S., McPhail, S. D., Perrett, J. R., Webb, A. T.,](#)
655 | [& White, D. \(2010\). Observations beneath Pine Island Glacier in West Antarctica and](#)
656 | [implications for its retreat. *Nature Geoscience*, 3\(7\), 468-472.](#)
- 657 | ~~14~~16. [Joughin, I., & Alley, R. B. \(2011\). Stability of the West Antarctic ice sheet in a](#)
658 | [warming world. *Nature Geoscience*, 4\(8\), 506-513.](#)
- 659 | ~~15~~17. [Kusahara, K., Hasumi, H. & Williams, G. D. \(2011\), Impact of the Mertz Glacier](#)
660 | [Tongue calving on dense water formation and export. *Nature communications*, 2, 159.](#)
- 661 | ~~16~~18. [Kern, S., & Spreen, G. \(2015\), Uncertainties in Antarctic sea-ice thickness](#)
662 | [retrieval from ICESat. *Annals of Glaciology*, 56\(69\), 107.](#)
- 663 | ~~17~~19. [Kwok, R., Cunningham, G. F., Zwally, H. J., & Yi, D. \(2007\). Ice, Cloud, and](#)
664 | [land Elevation Satellite \(ICESat\) over Arctic sea ice: retrieval of freeboard. *Journal of*](#)
665 | [Geophysical Research](#), 112, C12013, doi:10.1029/2006JC003978.
- 666 | ~~18~~20. [Legresy, B., Wendt, A., Tabacco, I. E., Remy, F., & Dietrich, R. \(2004\). Influence](#)
667 | [of tides and tidal current on Mertz Glacier, Antarctica. *Journal of Glaciology*, 50\(170\),](#)
668 | [427-435.](#)
- 669 | ~~19~~21. [Legresy, B., N. Young, L. Lescarmonier, R. Coleman, R. Massom, B. Giles, A.](#)
670 | [Fraser, R. Warener, B. Galton-Fenzi, L. Testut, M. Houssais and G. Masse \(2010\),](#)

Formatted: Font: Italic

671 CRAC!!! in the Mertz Glacier, Antarctica.
672 [http://www.antarctica.gov.au/__data/assets/pdf_file/0004/22549/ml_402353967939815_](http://www.antarctica.gov.au/__data/assets/pdf_file/0004/22549/ml_402353967939815_mertz_final_100226.pdf)
673 [mertz_final_100226.pdf](http://www.antarctica.gov.au/__data/assets/pdf_file/0004/22549/ml_402353967939815_mertz_final_100226.pdf)

674 ~~20,22.~~ Lescarmontier, L., Legr ́sy, B., Coleman, R., Perosanz, F., Mayet, C., & Testut, L.
675 (2012). Vibrations of Mertz glacier ice tongue, East Antarctica. *Journal of Glaciology*,
676 58(210), 665-676.

677 ~~21,23.~~ Ligtenberg, S. R. M., Heilsen, M. M., & van de Broeke, M. R. (2011). An
678 improved semi-empirical model for the densification of Antarctic firn. *The Cryosphere*,
679 5(4), 809-819.

680 ~~22,24.~~ Ligtenberg, S., Kuipers Munneke, P., & Van Den Broeke, M. R. (2014). Present
681 and future variations in Antarctic firn air content. *The Cryosphere*, 8(5), 1711-1723.

682 ~~23. Luckman, A., Padman, L., & Jansen, D. (2010). Persistent iceberg groundings in the~~
683 ~~western Weddell Sea, Antarctica. *Remote Sensing of Environment*, 114(2), 385-391.~~

684 ~~24,25.~~ Massom, R. A. (2003). Recent iceberg calving events in the Ninnis Glacier region,
685 East Antarctica. *Antarctic Science*, 15(02), 303-313.

686 ~~25,26.~~ Massom, R. A., Giles, A. B., Fricker, H. A., Warner, R. C., Legr ́sy, B., Hyland,
687 G., Young, N., & Fraser, A. D. (2010). Examining the interaction between multi-year
688 landfast sea ice and the Mertz Glacier Tongue, East Antarctica: Another factor in ice
689 sheet stability? *Journal of Geophysical Research*, 115, C12027,
690 doi:10.1029/2009JC006083.

691 ~~26,27.~~ Massom, R. A., Giles, A. B., Warner, R. C., Fricker, H. A., Legr ́sy, B., Hyland,
692 G., ... & Young, N. (2015). External influences on the Mertz Glacier Tongue (East

- 693 Antarctica) in the decade leading up to its calving in 2010. *Journal of Geophysical*
694 *Research: Earth Surface*, 120(3), 490-506.
- 695 ~~27-28.~~ Pavlis, N. K., Holmes S. A., Kenyon, S. C., & Factor, J. K. (2012). The
696 development and evaluation of the Earth Gravitational Model 2008 (EGM2008), *Journal*
697 *of Geophysical Research*. 117, B04406, doi:10.1029/2011JB008916.
- 698 ~~28-29.~~ Porter-Smith, R. (2003). Bathymetry of the George Vth Land shelf and slope.
699 *Deep Sea Research Part II: Topical Studies in Oceanography*, 50(8), 1337-1341.
- 700 ~~29. Post, A. L., Beaman, R. J., O'Brien, P. E., Eléaume, M., & Riddle, M. J. (2011).~~
701 ~~Community structure and benthic habitats across the George V Shelf, East Antarctica:~~
702 ~~trends through space and time. *Deep Sea Research Part II: Topical Studies in*~~
703 ~~*Oceanography*, 58(1), 105-118.~~
- 704 30. Pritchard, H. D., Ligtenberg, S. R. M., Fricker, H. A., Vaughan, D. G., Van den Broeke,
705 M. R., & Padman, L. (2012). Antarctic ice-sheet loss driven by basal melting of ice
706 shelves. *Nature*, 484(7395), 502-505.
- 707 31. Rignot, E., Mouginot, J. & Scheuchl, B. (2011), Ice flow of the Antarctic ice sheet.
708 *Science*, 333(6048), 1427-1430.
- 709 32. Rignot, E., & Jacobs, S. S. (2002). Rapid bottom melting widespread near Antarctic ice
710 sheet grounding lines. *Science*, 296(5575), 2020-2023.
- 711 33. Scambos, T. Hulbe, A., C. & Fahnestock, M. A. (2003). Climate-induced ice shelf
712 disintegration in the Antarctic Peninsula. *Antarctic Research Series*, 79, 79-92.
- 713 34. Scambos, T. Hulbe, A., C. Fahnestock, M. A. & Bohlander, J. (2000). The link between
714 climate warming and breakup of ice shelves in the Antarctic Peninsula. *Journal of*
715 *Glaciology*, 46(154), 516-530.

- 716 35. Shepherd, A., Wingham, D., Payne, T., & Skvarca, P. (2003). Larsen Ice Shelf has
717 progressively thinned. *Science*, 302(5646), 856-859.
- 718 ~~36. Smith, J., & Riddle, M. (2011). Benthic Community Survey, Mertz Glacier Region, East~~
719 ~~Antarctica: Post Survey Report, RSV Aurora Australis, Marine Science Voyage (2010/11~~
720 ~~VMS), January-February 2011. *Geoscience Australia*.~~
- 721 ~~37.~~36. Smith, K. L., Robison, B. H., Helly, J. J., Kaufmann, R. S., Ruhl, H. A., Shaw, T.
722 J., ... & Vernet, M. (2007). Free-drifting icebergs: hot spots of chemical and biological
723 enrichment in the Weddell Sea. *Science*, 317(5837), 478-482.
- 724 ~~38.~~37. Smith, K. L. (2011). Free-drifting icebergs in the Southern Ocean: an overview.
725 *Deep Sea Research Part II: Topical Studies in Oceanography*, 58(11), 1277-1284.
- 726 ~~39.~~38. Tamura, T., Williams, G. D., Fraser, A. D. & Ohshima, K. I. (2012). Potential
727 regime shift in decreased sea ice production after the Mertz Glacier calving, *Nature*
728 *communications*, 3, 826.
- 729 ~~40.~~39. Tchernia, P. A. U. L., & Jeannin, P. F. (1984). Circulation in Antarctic waters as
730 revealed by iceberg tracks 1972–1983. *Polar Rec*, 22(138), 263-269.
- 731 ~~41.~~40. Van de Berg, W. J., Van den Broeke, M. R., Reijmer, C. H., & Van Meijgaard, E.
732 (2005). Characteristics of the Antarctic surface mass balance, 1958–2002, using a
733 regional atmospheric climate model. *Annals of glaciology*, 41(1), 97-104.
- 734 ~~42.~~41. Van de Berg, W. J., Van den Broeke, M. R., Reijmer, C. H., & Van Meijgaard, E.
735 (2006). Reassessment of the Antarctic surface mass balance using calibrated output of a
736 regional atmospheric climate model. *Journal of Geophysical Research: Atmospheres*
737 (1984–2012), 111(D11).

- 738 | ~~43-42.~~ Van den Broeke, M. (2008). Depth and density of the Antarctic firm layer. *Arctic,*
739 | *Antarctic, and Alpine Research*, 40(2), 432-438.
- 740 | ~~44-43.~~ Wang, X.W., Cheng, X., Gong, P., Huang, H. B., Li Z., & Li, X. W. (2011). Earth
741 | Science Applications of ICESat/GLAS: a Review. *International Journal of Remote*
742 | *Sensing*, 32, 23, 8837-8864, doi: 10.1080/01431161.2010.547533
- 743 | ~~45-44.~~ Wang, X.W., Cheng, X., Gong, P., Shum, C. K., Holland, D.M., & Li, X.W.
744 | (2014). Freeboard and mass extraction of the disintegrated Mertz Ice Tongue with remote
745 | sensing and altimetry data. *Remote Sensing of Environment*, 144, 1-10.
- 746 | 45. Wang, X.W. (2014). Mertz ice tongue evolutions from satellite observed data,
747 | Postdoctoral Research Report, College of Global Change and Earth System Science,
748 | Beijing Normal University, China. doi: 10.13140/2.1.1006.1603
- 749 | 46. Wang, X., Cheng, X., Li, Z., Huang, H., Niu, Z., Li, X., & Gong, P. (2012). Lake water
750 | footprint identification from time-series ICESat/GLAS data. *Geoscience and Remote*
751 | *Sensing Letters, IEEE*, 9(3), 333-337.
- 752 | 47. Wang, X., Gong, P., Zhao, Y., Xu, Y., Cheng, X., Niu, Z., ... & Li, X. (2013). Water-
753 | level changes in China's large lakes determined from ICESat/GLAS data. *Remote Sensing*
754 | *of Environment*, 132, 131-144.
- 755 | ~~46-~~
- 756 | ~~47-48.~~ Woodworth-Lynas, C. M. T., Josenhans, H. W., Barrie, J. V., Lewis, C. F. M., &
757 | Parrott, D. R. (1991). The physical processes of seabed disturbance during iceberg
758 | grounding and scouring. *Continental Shelf Research*, 11(8), 939-961.

Formatted: Font: Italic

Formatted: Font: Italic

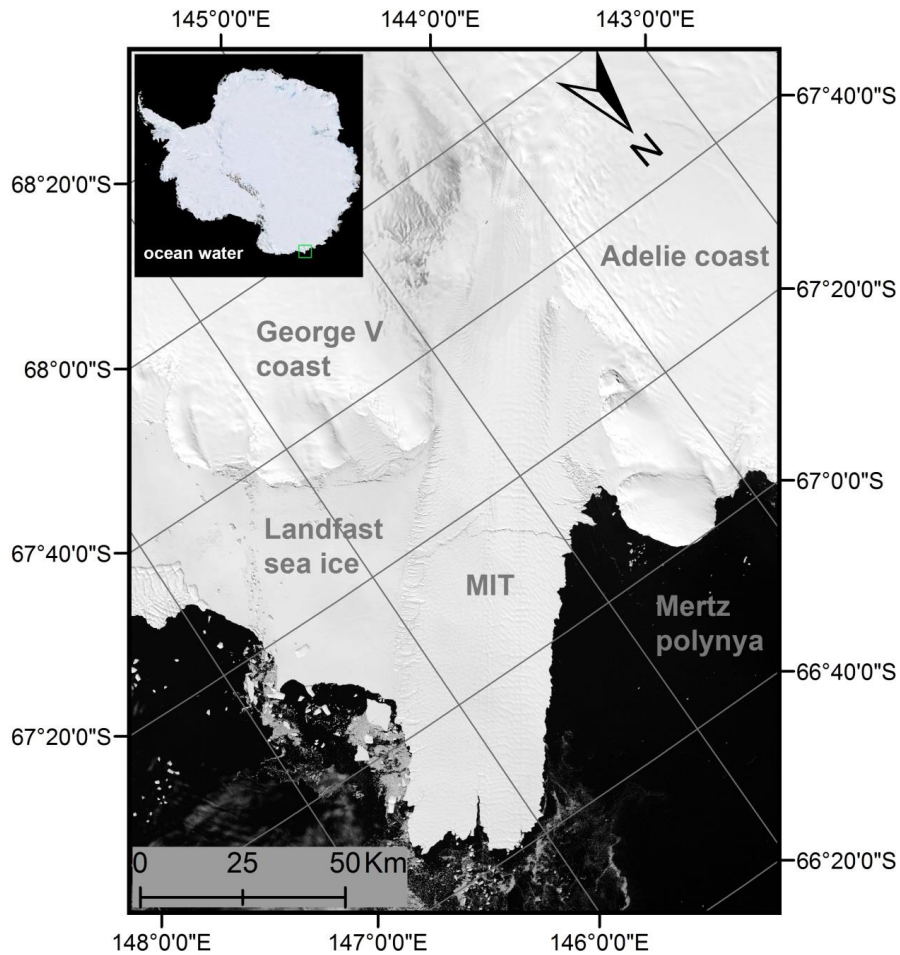
759 | ~~48~~49. Yi, D., Zwally, H.J., & Robbins, J. (2011). ICESat observations of seasonal and
760 | interannual variations of sea-ice freeboard and estimated thickness in the Weddell Sea,
761 | Antarctica (2003-2009). *Annals of Glaciology*, 52(57), 43-51.

762 | ~~49~~50. Zwally, H. J., Schutz, B., Abdalati, W., Abshire, J., Bentley, C., Brenner, A.,
763 | Buftona, J., Deziouf, J., Hancocka, D., Hardinga, D., Herringg, T., Minsterh, B.,
764 | Quinng, K., Palmi, S., Spinhirnea, J., & Thomasj, R. (2002). ICESat's laser
765 | measurements of polar ice, atmosphere, ocean, and land. *Journal of Geodynamics*, 34,
766 | 405-445.

767 | ~~50~~51. Zwally, H. J., Yi, D., Kwok, R., & Zhao, Y. (2008). ICESat measurements of sea
768 | ice freeboard and estimates of sea ice thickness in the Weddell Sea. *Journal of*
769 | *Geophysical Research*, 113, C02S15, doi:10.1029/2007JC004284.

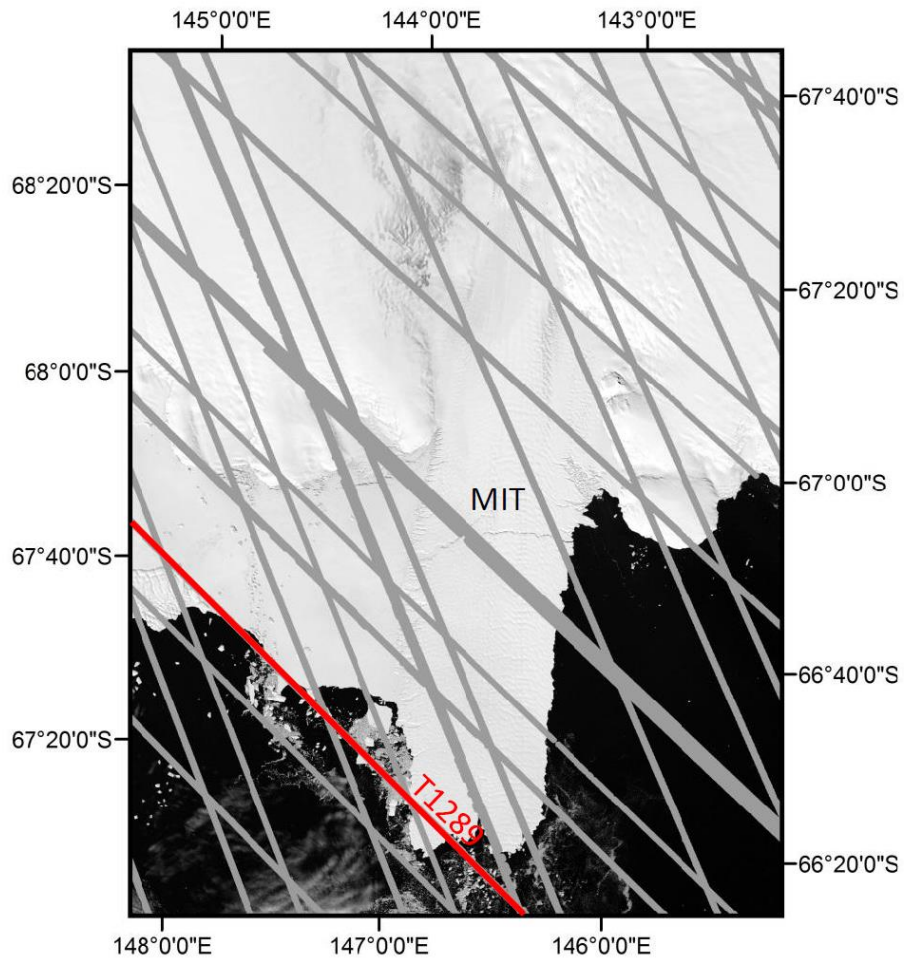
770

Figures

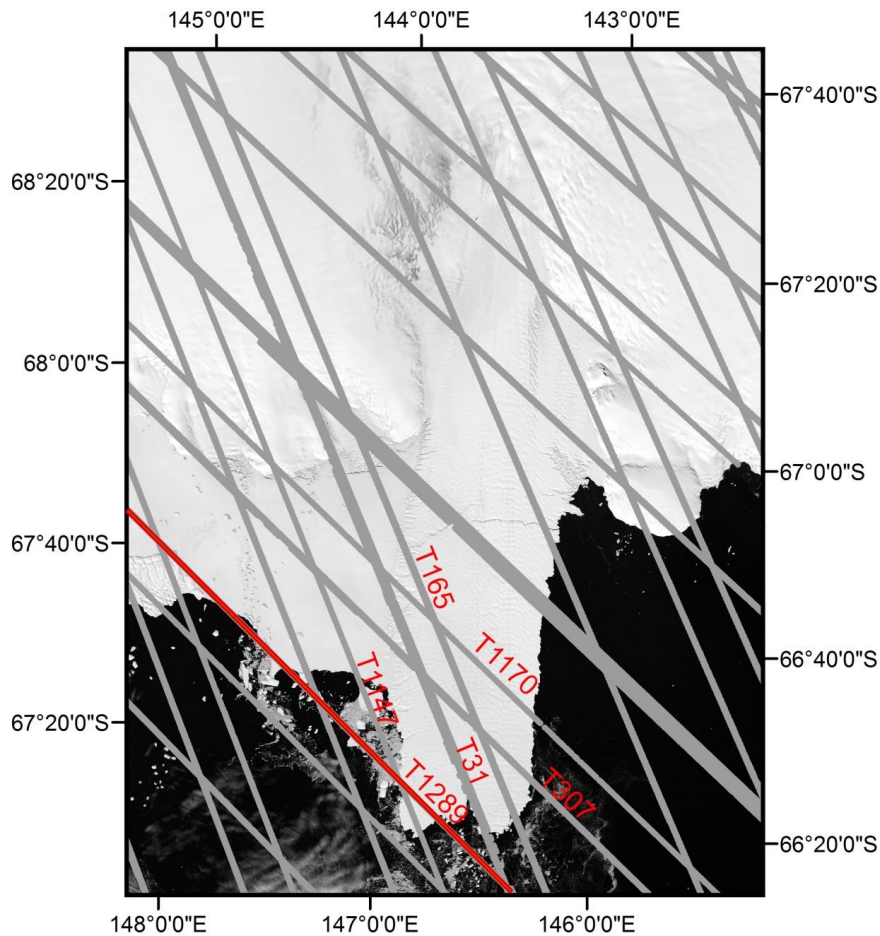


772

773 **Figure 1.** Mertz Ice Tongue (MIT), East Antarctica. Landfast sea ice is attached to the east flank
 774 of the MIT and the Mertz Polynya is to the west. The background image is from band 4 Landsat
 775 7, captured on February 2, 2003. The green square found in the upper left inset indicates the
 776 location of the MIT in East Antarctica. A polar stereographic projection with -71°S as standard
 777 latitude is used.

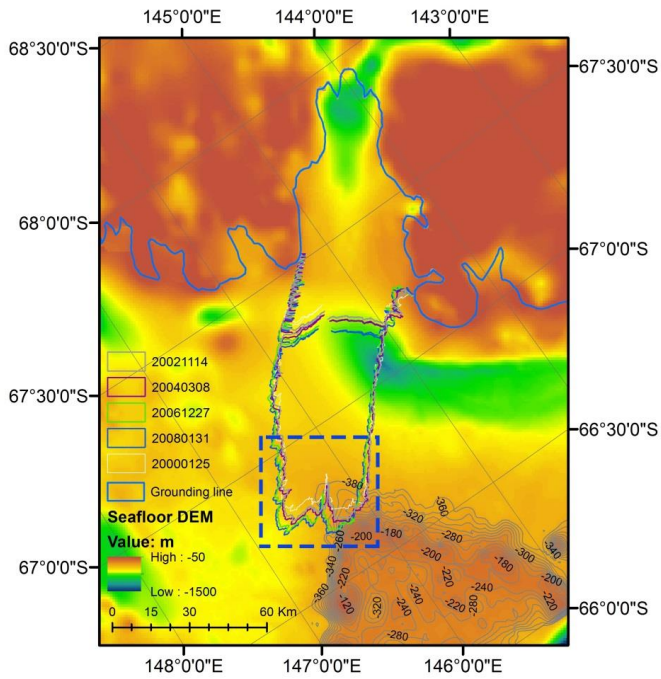
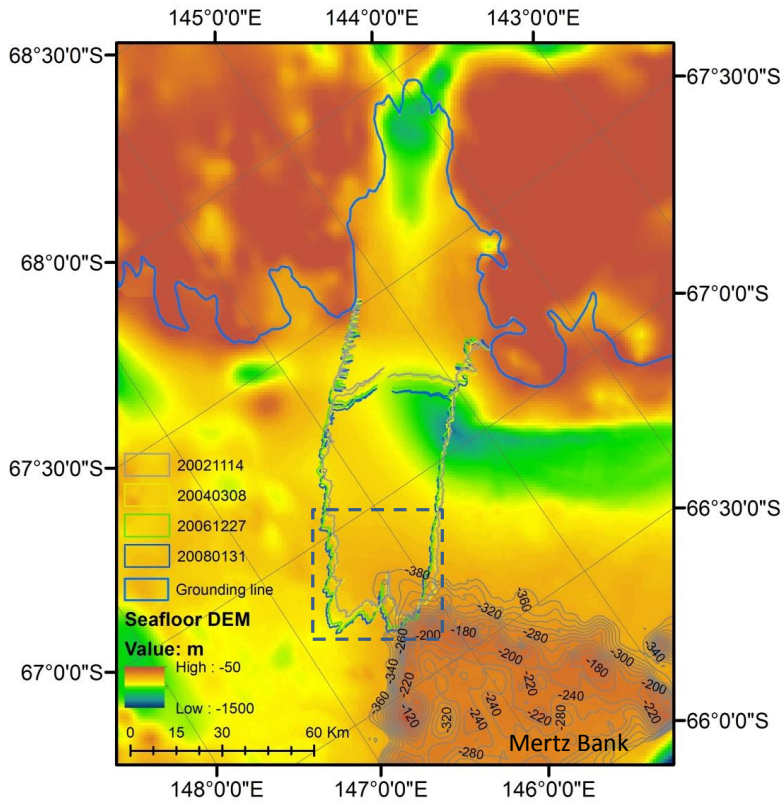


778

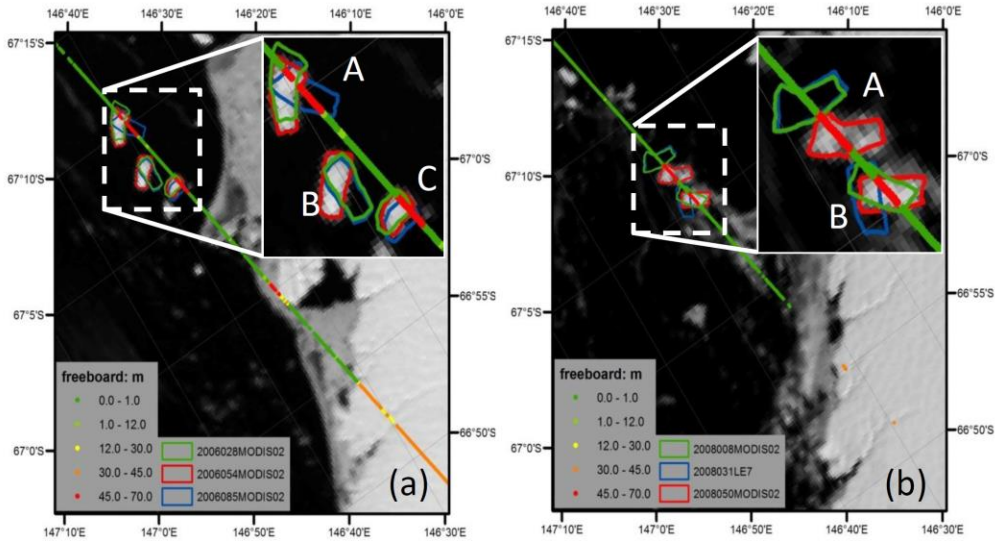


779

780 **Figure 2.** Spatial distribution of ICESat/GLAS data from 2003 to 2009 covering the Mertz
781 region. Ground tracks of ICESat/GLAS are indicated with gray lines. Track 1289 (T1289) is
782 highlighted in red as is used in [Figure-Fig. 64](#). The background image is from band 4 Landsat 7,
783 captured on February 2, 2003. A polar stereographic projection with -71 °S as standard latitude is
784 used.



786 **Figure 3.** Seafloor topography from bathymetry around Mertz region and outlines of the MIT
787 from 2002 to 2008. The outlines of the MIT in different years are marked with different colored
788 polygons. The shallow Mertz Bank is located in the lower right (northeast). The blue inset box
789 corresponds to location of Figure-Fig. 46 and 7. The bathymetry measurement profile can be
790 found from S-Figure-Fig. 1.

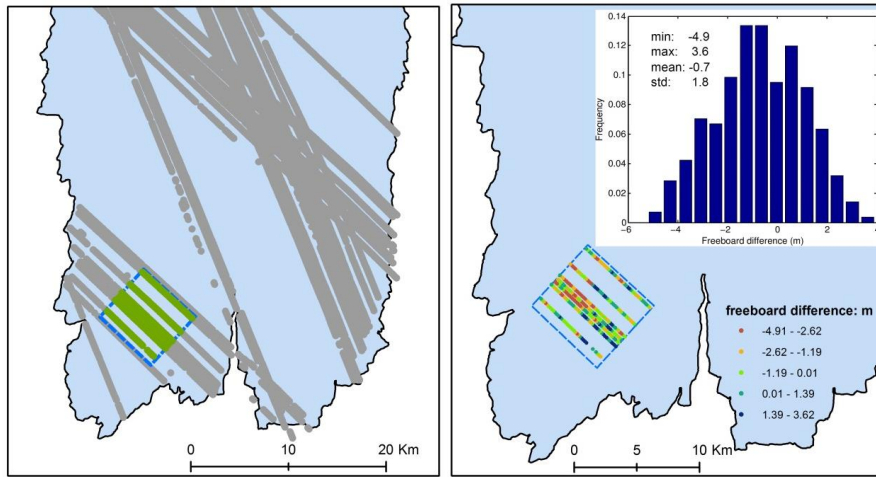


791

792 **Figure 4.** Freeboard extracted from Track 1289, ICESat/GLAS, the location of which can be
 793 found in [Figure-Fig. 2](#) and [S-Figure-Fig. 1](#). (a) and (b) show the freeboard extracted from
 794 ICESat/GLAS on February 23, 2006 (2006054) and February 18, 2008 (2008049) respectively.
 795 In each image, positions of three icebergs (with name labeled as ‘A’, ‘B’ and ‘C’) ~~elosed~~closest
 796 to ICESat/GLAS observation time are plotted with green, red and blue polygons respectively.
 797 The dates are indicated with seven numbers (yyyyddd) in legend. ‘yyyyddd’ stands for day ‘ddd’
 798 in year ‘yyyy’. ‘MODIS02’ and ‘LE7’ indicate that the image used to extract iceberg outline is
 799 from MODIS and Landsat 7 ETM+, respectively.

800

801



(a) (b)

802

803

804

805

806

807

808

809

810

811

812

813

814

Figure 5. Evaluation of kriging interpolation method over the MIT using freeboard data derived from ICESat/GLAS. (a) is freeboard data derived from ICESat/GLAS after relocation over the MIT. Gray dots indicate ICESat/GLAS used for interpolation using kriging method. The blue dashed square indicates the region used to investigate interpolation accuracy of kriging method, about 7 km×7 km. Inside of the square, freeboard data marked with green dots are used to check the accuracy of freeboard interpolated with kriging. (b) is the freeboard comparison result derived by subtracting krigged freeboard from freeboard derived from ICESat/GLAS. The spatial distribution and the histogram of freeboard difference is shown in the lower left and upper right respectively. The black polygon filled with light blue shows the boundary of MIT on November 14, 2002.

Formatted: Font: (Default) Times New Roman, 12 pt

Formatted: Font: (Default) Times New Roman, 12 pt, Bold

Formatted: Font: (Default) Times New Roman, 12 pt

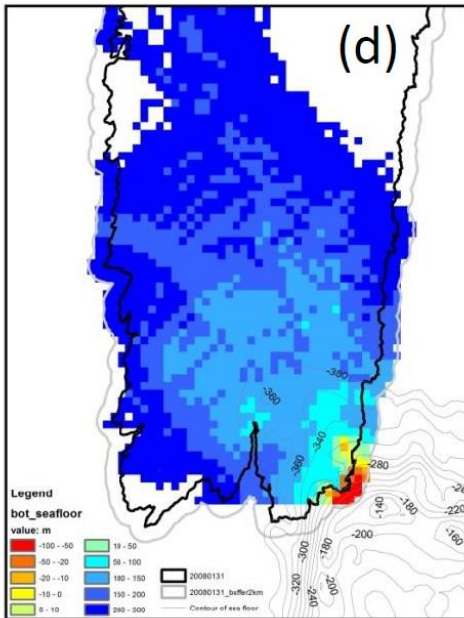
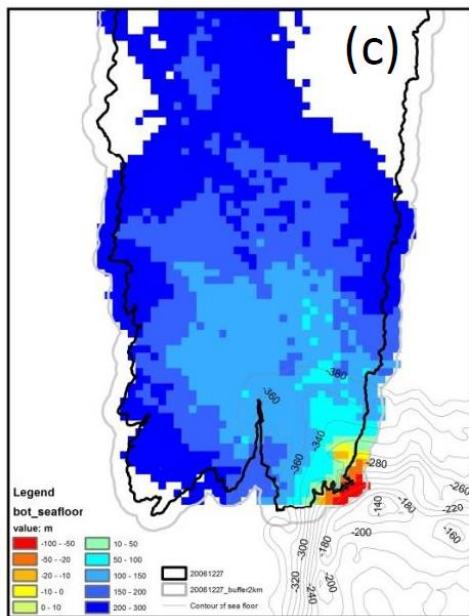
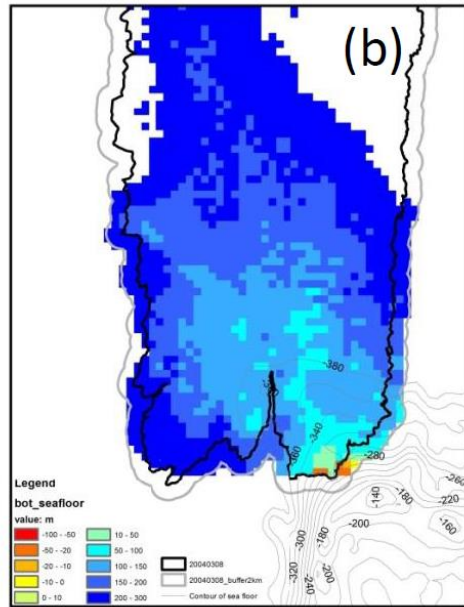
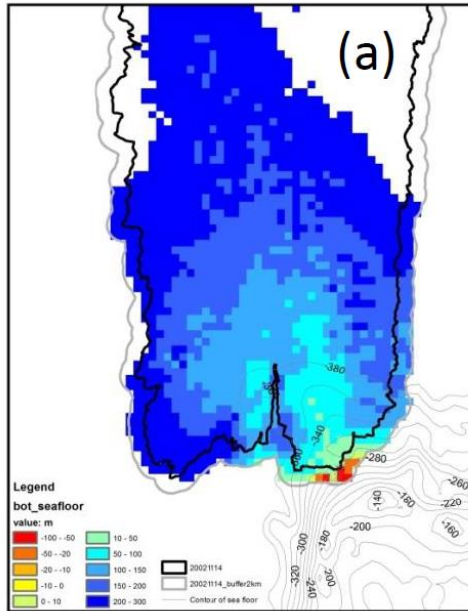
Formatted: Left, Line spacing: Double

Formatted: Font: (Default) Times New Roman, 12 pt

Formatted: Font: (Default) Times New Roman, 12 pt

Formatted: Font: (Default) Times New Roman, 12 pt

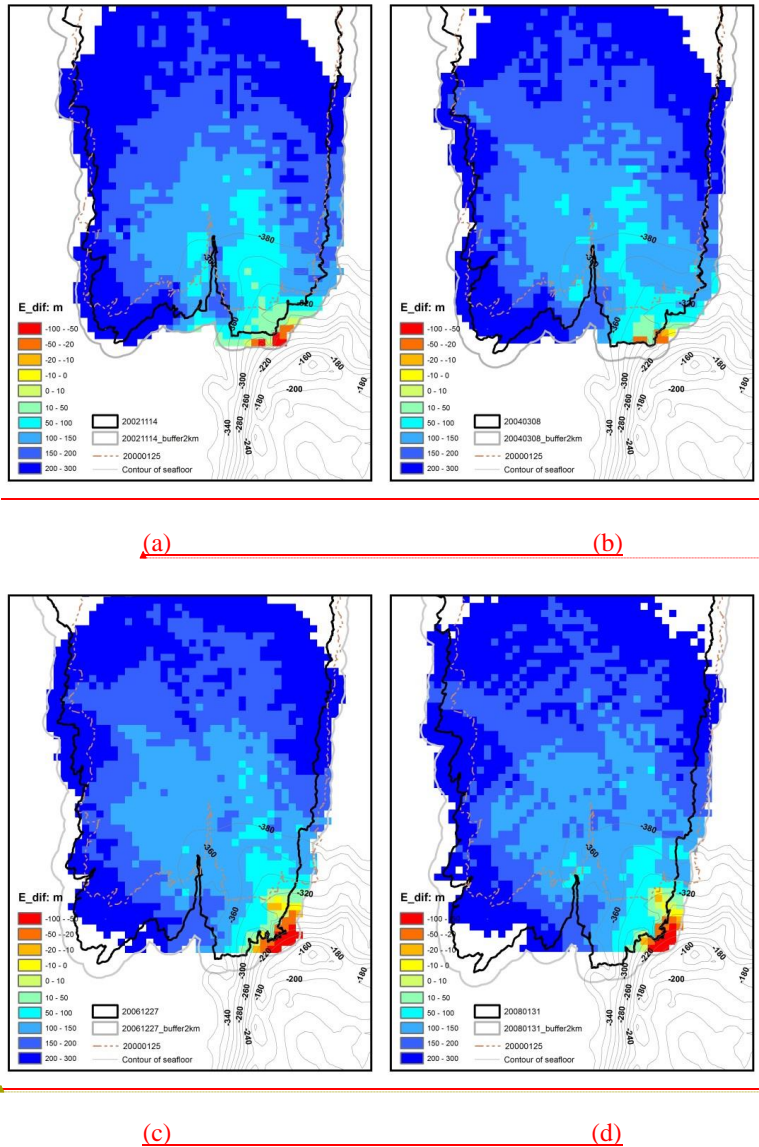
Formatted: Font: (Default) Times New Roman, 12 pt



815

816

817
818



Formatted: Font: (Default) Times New Roman, 12 pt

Formatted: Font: (Default) Times New Roman, 12 pt

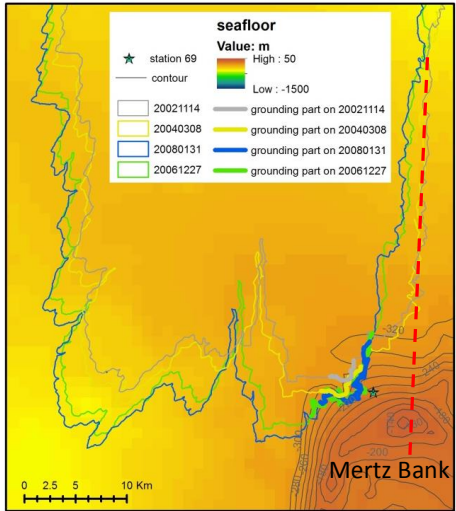
Formatted: Font: (Default) Times New Roman, 12 pt

819
820
821

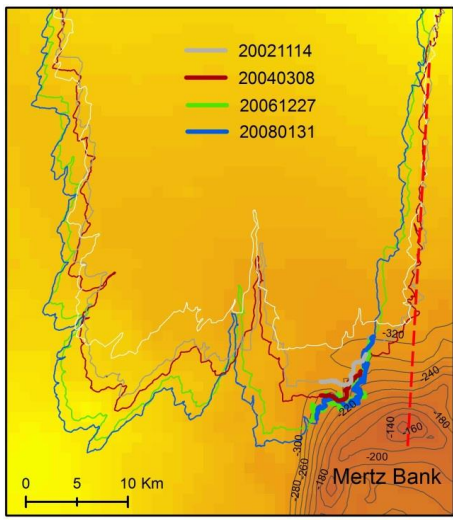
822 **Figure 56.** Elevation difference of Mertz ice bottom and seafloor topography. (a), (b), (c) and (d)
823 correspond to elevation difference assuming hydrostatic equilibrium under the minimum sea

824 surface height -3.35 m on November 14, 2002 , March 8, 2004, December 27, 2006, and January
825 31, 2008, respectively. The contours in the lower right indicate seafloor topography (unit: m) of
826 the Mertz Bank with an interval of 20 m. The solid black line indicates the boundary of the MIT
827 and the thick gray line outlines a buffer region of the boundary with 2 km as buffer radius. The
828 dashed line indicates the shape of the MIT on January 25, 2000, which is used to identify the
829 bathymetry gap under the ice tongue. In the legend, negative values mean that ice bottom is
830 lower than the seafloor, which of course is impossible. Therefore, the initial assumption of a
831 floating ice tongue was incorrect in those locations (yellow to red colors), and the ice was
832 grounded. Regions with more negative values indicate more heavily grounding inside of the MIT
833 or more heavily grounding potential in the buffer region.

834

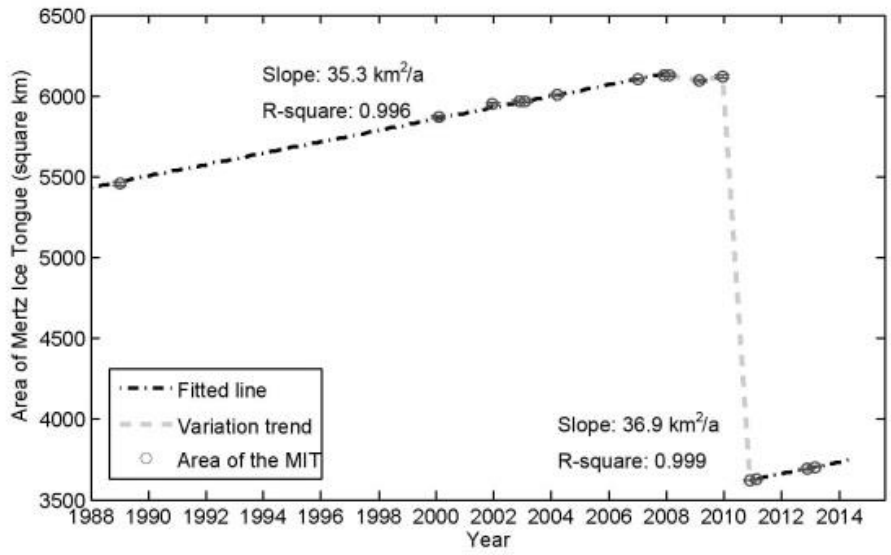


835



836 **Figure 67.** Digital Elevation Map (DEM) of seafloor around Mertz and grounding section of the
837 boundaries extracted from 2002 to 2008. Grounding section of MIT boundary in 2002, 2004,
838 2006 and 2008 is marked with thick gray, purple, green and blue polylines respectively and MIT
839 boundaries are indicated with polygons with the same legend as Fig. 3. Additionally, MIT

840 | boundary in 2000 indicated with white polygon is used to show the different quality of seafloor
841 | DEM. Inside of this polygon no bathymetry data was collected or used. The dashed red line
842 | indicates the 'extension line' of the west flank of MIT on November 14, 2002, passing the
843 | shallowest region of the Mertz Bank (about -140 m).

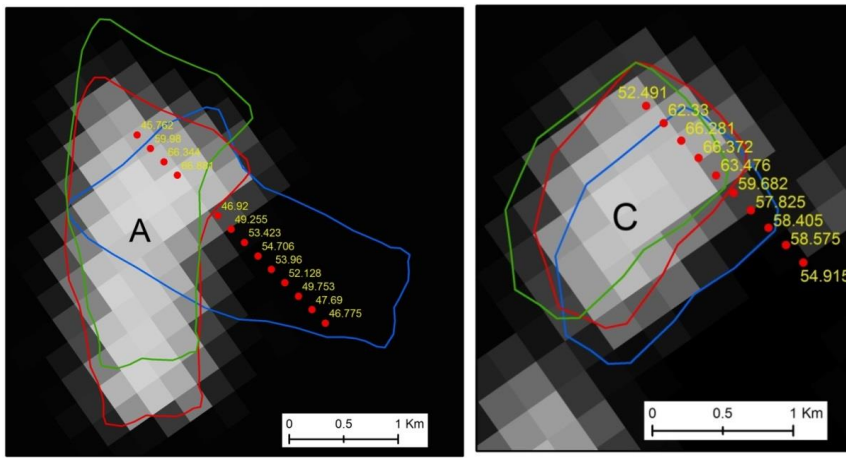


844

845 **Figure 78.** Time series of area change of the MIT. The area covers the entire ice tongue, to the
 846 grounding line as indicated with thick blue line in [Figure Fig. 3](#). The area is extracted from
 847 Landsat images from 1988 to 2013.

848

849

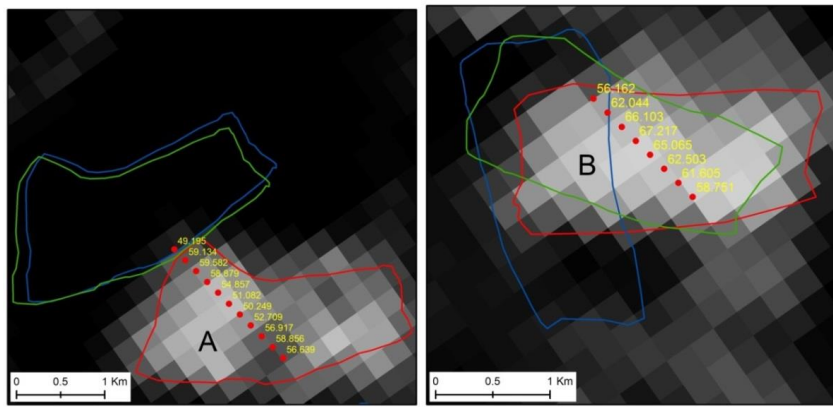


(a) (b)

Formatted: Centered

850

851



(c) (d)

Formatted: Centered

852

853

854 **Figure 9.** Freeboard extraction results from ICESat/GLAS for icebergs ‘A’, ‘B’ and ‘C’ in 2006
 855 and 2008 respectively. (a) and (b) correspond to freeboard measurements from ‘A’ and ‘C’
 856 respectively on February 23, 2006 (2006054), with background image from MODIS captured on
 857 2006054. (c) and (d) correspond to freeboard measurements from ‘A’ and ‘B’ respectively on
 858 February 18, 2008 (2008049), with background image from MODIS captured on 2008050. The

Formatted: Font: Bold

859 location of each iceberg in different observation time is indicated with different colored polygons,
860 the legend of which is the same as what is used in Fig. 4. Inside of each sub-figure, different
861 icebergs are marked with capital characters 'A', 'B' and 'C' respectively and iceberg freeboard
862 results in unit of meter are marked in yellow.

863

Tables

864 **Table 1.** Statistics of the three icebergs used to inverse FAC with least-square method. Icebergs865 ‘A’, ‘B’ and ‘C’ are the same as what are used in Fig. 4 [and 9. Measurements from icebergs ‘A’](#)866 [and ‘C’ in February 2006 are used to derive FAC with least-squares method. Icebergs ‘A’ and ‘B’](#)867 [in 2008 are used for validation.](#)

<u>Icebergs</u>	<u>date</u>	<u>Latitude</u> (°)	<u>Longitude</u> (°)	<u>Freeboard</u> (m)	<u>Seafloor</u> (m)	<u>Sea level</u> (m)	ϵ (m)	E_{dif} (m)
A	Feb 23, 2006	-67.1737	146.6595	66.88	-528.48	-1.92	0.89	
		-67.1752	146.6604	66.34	-527.01	-1.92	1.30	
C	Feb 23, 2006	-67.1085	146.6247	66.37	-505.84	-1.92	-1.25	
		-67.1100	146.6255	66.28	-507.08	-1.92	-1.01	
A	Feb 18, 2008	-67.1194	146.6303	58.88	-522.52	-2.08		69.14
		-67.1209	146.6311	59.58	-524.16	-2.08		64.88
B	Feb 18, 2008	-67.0906	146.6151	67.22	-500.92	-2.08		-22.45
		-67.0921	146.6159	66.10	-500.47	-2.08		-13.55
<u>Icebergs</u>	<u>date</u>	<u>Latitude</u> (°)	<u>Longitude</u> (°)	<u>Freeboard</u> (m)	<u>Seafloor</u> (m)	<u>Sea level</u> (m)	E_{arf} (m)	
A	Feb 23, 2006	-67.1737	146.6595	66.88	-528.48	-1.92	7.93	
		-67.1752	146.6604	66.34	-527.01	-1.92	10.96	
C	Feb 23, 2006	-67.1085	146.6247	66.37	-505.84	-1.92	-10.44	
		-67.1100	146.6255	66.28	-507.08	-1.92	-8.44	
A	Feb 18, 2008	-67.1194	146.6303	58.88	-522.52	-2.08	69.14	
		-67.1209	146.6311	59.58	-524.16	-2.08	64.88	

B	Feb 18, 2008	-67.0906	146.6151	67.22	-500.92	-2.08	-22.45
		-67.0921	146.6159	66.10	-500.47	-2.08	-13.55

868

869 **Table 2.** Statistics of grounding grids inside or grounding potentials outside of the Mertz Ice
870 Tongue (MIT) (‘I’: inside of thick black line, Fig. 56; Number in brackets indicates how many
871 grids are located inside of the 2000 Mertz boundary. ‘O’: between the black and gray lines, Fig.
872 56) on November 14, 2002, March 8, 2004, December 27, 2006 and January 31, 2008
873 respectively. Each grid covers an area of 1 km². The Mean, Minimum and Standard deviation is
874 calculated without considering those fallen inside of the 2000 Mertz boundary, but only those
875 having elevation difference less than 46 m and out of 2000 Mertz boundary.

Elevation difference (subtracting seafloor from ice bottom)	2002-11-14		2004-03-08		2006-12-27		2008-01-31	
	I	O	I	O	I	O	I	O
17-34(m)	4	5	4	2	7	1	3	5
0-17(m)	2	6	1	1	6	2	4	2
<0(m)	0	8	2	5	7	21	6	18
Mean (m)	25.0	-11.9	8.9	-6.4	3.8	-42.1	-0.8	-31.0
Minimum (m)	11.9	-81.5	-46.0	-44.5	-52.3	-102.8	-34.8	-103.0
Standard deviation (m)	8.4	37.8	28.0	27.1	21.8	36.4	19.9	38.0
Number of grids	6	19	7	8	20	22	13	25

Formatted Table

Formatted Table

Formatted Table

876

Elevation difference (subtracting seafloor from ice bottom)	2002-11-14		2004-03-08		2006-12-27		2008-01-31	
	I	O	I	O	I	O	I	O
23-46 (m)	9(3)	10(0)	6(0)	3(0)	10(1)	1(0)	10(3)	5(0)
0-23 (m)	2(0)	6(0)	1(0)	1(0)	9(0)	2(0)	4(0)	2(0)
<0 (m)	0(0)	8(0)	2(0)	5(0)	7(0)	21(0)	6(0)	18(0)
Mean (m)	28.8	9.8	15.8	-1.1	10.9	-41.9	12.3	-31.0
Minimum (m)	11.9	-81.5	-46.0	-44.5	-52.3	-102.8	-34.8	-103.0

<u>Standard deviation (m)</u>	<u>9.2</u>	<u>36.8</u>	<u>29.6</u>	<u>31.4</u>	<u>24.7</u>	<u>37.6</u>	<u>27.3</u>	<u>38.0</u>
<u>Number of grids</u>	<u>8</u>	<u>24</u>	<u>9</u>	<u>9</u>	<u>25</u>	<u>24</u>	<u>17</u>	<u>25</u>

877

878 **Table 3.** Statistics of grounding outlines of the MIT as shown with thick polylines in Fig. 6-7 on
 879 November 14, 2002, March 8, 2004, December 27, 2006 and January 31, 2008 respectively

	2002-11-14	2004-03-08	2006-12-27	2008-01-31
Start location (°)	146. 160 <u>124</u> °E, 66. 689 <u>696</u> °S	146.155 °E, 66.681 °S	146.093 °E, 66.700 °S	146. 108 <u>088</u> °E, 66. 695 <u>699</u> °S
End location (°)	146. 222 <u>240</u> °E, 66. 689 <u>693</u> °S	146.256 °E, 66.683 °S	146.304 °E, 66.669 °S	146. 271 <u>292</u> °E, 66. 675 <u>668</u> °S
Perimeter (km)	4.27 <u>0</u>	6.4	24.7	18.02 <u>0.9</u>

880